

# Investigation of the role of miRNA targeting NFAT as a biomarker of Myocardial Infarction



*By*

**Wishma Seher**

**Department of Biochemistry  
Faculty of Biological Sciences  
Quaid-i-Azam University  
Islamabad, Pakistan  
2023**

# **Investigation of the role of miRNA targeting NFAT as a biomarker of Myocardial Infarction**



A dissertation submitted in the fulfillment of requirements for the

**Degree of Master of Philosophy In**

**Biochemistry/ Molecular Biology**

*By*

**Wishma Seher**

**Department of Biochemistry  
Faculty of Biological Sciences  
Quaid-i-Azam University  
Islamabad, Pakistan  
2023**

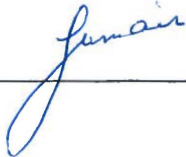
بِسْمِ اللَّهِ الرَّحْمَنِ الرَّحِيمِ

## CERTIFICATE

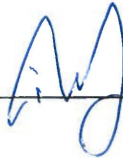
This thesis, submitted by **Ms. Wishma Seher** to the Department of Biochemistry, Faculty of Biological Sciences, Quaid-i-Azam University, Islamabad, Pakistan, is accepted in its present form as satisfying the thesis requirement for the Degree of Master of Philosophy in Biochemistry/Molecular Biology.

**Examination Committee:**


1. **External Examiner:**  
**Dr. Sumaira Farrakh**  
Associate Professor  
Department of Bioscience,  
COMSATS, University Islamabad

Signature:  \_\_\_\_\_

2. **Supervisor:**  
**Prof. Dr. Iram Murtaza**

Signature:  \_\_\_\_\_

3. **Chairperson:**  
**Prof. Dr. Iram Murtaza**

Signature:  \_\_\_\_\_

**Dated:**

**November 02, 2023**

## **DECLARATION**

I affirm that this thesis is the result of my individual endeavors and diligent work. I assert my full authorship of this work and confirm that I have not previously presented it to attain any academic qualification. The data in this thesis is confidential and is currently under patent review.

**Wishma Seher**

*This thesis is dedicated to my family.*

*In recognition of their boundless affection, unwavering support, and  
motivating influence.*

## ACKNOWLEDGEMENT

In the pursuit of knowledge and the crafting of this thesis, I am profoundly grateful to **Allah** ﷻ, The Lord of the universe, The Most Beneficent and The Merciful, for bestowing His boundless blessings upon me. His guidance and support have enabled me to contribute to the field of knowledge and encapsulate my endeavors within these pages. I extend heartfelt salutations to The **Holy Prophet, Hazrat Muhammad** ﷺ, whose wisdom serves as a beacon of knowledge and guidance for all of humanity.

At this juncture, I wish to express my sincere appreciation to **Dr. Iram Murtaza**, my research supervisor and chairperson of the Department of Biochemistry. Her unwavering interest, encouragement, dedication, and scholarly guidance have been instrumental in shaping the trajectory of this research, guiding me towards the fulfillment of my academic aspiration.

My gratitude extends to my esteemed lab seniors, **Aqsa Naeem, Aamna Sayeed, Syeda Laiba Tayyab, Khadam Hussain**, and, in particular, my mentor **Ayesha Ishtiaq**. They all have been very cooperative and supportive in my research journey.

A big thank you goes out to my dear friends and colleagues, **Bushra Khalid, Mahnoor Sakina, Palwasha Iqbal, Irum Nasir, Mirub Shaukat, and Alina Murtaza**. They provided me with encouragement and steadfastly stood by my side throughout this journey.

I can't thank my **family** enough, especially my siblings **Wishal Mehmood** and **Isha Emaan**. Their prayers, love, and care gave me the strength and hope to finish this task and work towards my goals. Their support means more than words can say. I extend my sincere appreciation to all those who offered their support, whether through direct guidance, uplifting words, or silent blessings. Your diverse contributions have been vital in shaping the culmination of this thesis.

## TABLE OF CONENTS

List of Abbreviations .....	i
List of Figures .....	v
List of Tables .....	vii
Abstract .....	viii
<b>1. Introduction.....</b>	<b>1</b>
<b>1.1. Cardiovascular diseases.....</b>	<b>1</b>
<b>1.2. Myocardial Infarction.....</b>	<b>1</b>
<b>1.3. Coronary Artery Disease.....</b>	<b>1</b>
<b>1.3.1. Risk factors .....</b>	<b>2</b>
<b>1.3.2. Oxidative stress.....</b>	<b>2</b>
<b>1.3.3. Sources of ROS in cardiac cells.....</b>	<b>3</b>
<b>1.3.4. Types of ROS in cardiac cells.....</b>	<b>3</b>
<b>1.3.5. Antioxidant defense system .....</b>	<b>4</b>
<b>1.4. Major events in CAD development.....</b>	<b>4</b>
<b>1.5. Biogenesis of miRNA.....</b>	<b>6</b>
<b>1.6. Action of miRNA .....</b>	<b>7</b>
<b>1.6.1. Dysregulated miRNAs in CAD.....</b>	<b>8</b>
<b>1.6.2. Target genes .....</b>	<b>9</b>
<b>1.7. Stages of CAD development .....</b>	<b>11</b>
<b>1.9. Diagnosis of CAD .....</b>	<b>14</b>
<b>1.10. Aims And Objectives.....</b>	<b>15</b>
<b>2. MATERIALS AND METHODS .....</b>	<b>16</b>
<b>2.1. Study Hypothesis .....</b>	<b>16</b>
<b>2.2. Study Design.....</b>	<b>16</b>
<b>2.3. Ethical considerations .....</b>	<b>16</b>
<b>2.4. Sample collection .....</b>	<b>17</b>



<b>2.5.</b>	<b>Dose regimen and sample collection from Sprague Dawley Rats</b> .....	17
<b>2.6.</b>	<b>Tissue homogenization</b> .....	18
<b>2.6.1.</b>	<b>Lysis buffer</b> .....	18
<b>2.7.</b>	<b>Protein Quantification using Bradford Assay</b> .....	19
<b>2.8.</b>	<b>Western Blotting</b> .....	20
<b>2.8.1.</b>	<b>Preparation of the gel</b> .....	21
<b>2.8.2.</b>	<b>Sample preparation and electrophoretic separation of the proteins</b> 21	
<b>2.8.3.</b>	<b>Sample Loading and Gel Running</b> .....	22
<b>2.8.4.</b>	<b>Gel Staining</b> .....	23
<b>2.8.5.</b>	<b>Transfer of Proteins on Nitrocellulose Membrane</b> .....	24
<b>2.8.6.</b>	<b>Blocking</b> .....	26
<b>2.8.7.</b>	<b>Antibody Treatment</b> .....	26
<b>2.8.8.</b>	<b>Chromogenic Detection</b> .....	27
<b>2.9.</b>	<b>Quantitative Real Time PCR Analysis</b> .....	27
<b>2.9.1.</b>	<b>RNA extraction</b> .....	28
<b>2.9.2.</b>	<b>RNA Quantification</b> .....	29
<b>2.9.3.</b>	<b>cDNA Synthesis</b> .....	29
<b>2.9.4.</b>	<b>cDNA dilution</b> .....	30
<b>2.9.5.</b>	<b>Real Time Polymerase Chain Reaction (qRT-PCR/RT-qPCR)</b> .....	30
<b>2.10.</b>	<b>Fluorescence-based miRNA quantification</b> .....	31
<b>2.11.</b>	<b>Oxidative Profiling</b> .....	31
<b>2.11.1.</b>	<b>Reactive Oxygen Species (ROS) Assay</b> .....	31
<b>2.11.2.</b>	<b>Thio-barbituric acid Reactive substances (TBARs) level</b> .....	32
<b>2.12.</b>	<b>Estimation of Antioxidative Profile</b> .....	33
<b>2.12.1.</b>	<b>Super Oxide Dismutase (SOD) Assay</b> .....	33
<b>2.12.2.</b>	<b>Catalase Activity (CAT) Assay</b> .....	34

2.12.3.	<b>Peroxidase (POD) Assay</b> .....	34
2.12.4.	<b>Ascorbate Peroxidase (APX) Assay</b> .....	35
2.12.5.	<b>Reduced Glutathione Assay</b> .....	36
2.13.	<b>Lipid profile</b> .....	36
2.13.1.	<b>Cholesterol assay</b> .....	36
2.13.2.	<b>Triglycerides</b> .....	37
2.14.	<b>Liver function tests</b> .....	38
2.14.1.	<b>Alanine Aminotransferase (ALT) Assay</b> .....	38
2.14.2.	<b>Aspartate Aminotransferase (AST) assay</b> .....	39
2.15.	<b>Statistical Analysis</b> .....	40
2.16.	<b>Histopathology</b> .....	40
2.16.1.	<b>Microtomy</b> .....	40
2.16.2.	<b>Microscopic Analysis</b> .....	40
3.	<b>RESULTS</b> .....	41
3.1.	<b>Research Summary</b> .....	41
3.2.	<b>Demographic Data of Patients</b> .....	41
3.2.1.	<b>Gender-wise Distribution</b> .....	41
3.2.2.	<b>Age-wise Distribution</b> .....	42
3.2.3.	<b>Other Diseases in CAD Patients</b> .....	42
3.2.4.	<b>Smoking Status in CAD Patients</b> .....	43
3.3.	<b>Relative expression analysis of miRNAs and target genes in CAD Patients</b> 44	
3.3.1.	<b>Increased expression of miR-1-3p in CAD Patients</b> .....	44
3.3.2.	<b>Decreased expression of miR-98-5p in CAD Patients</b> .....	44
3.3.3.	<b>mRNA expression analysis of genes as putative miRNA targets</b> .....	45
3.3.4.	<b>Reduced expression of NFATc3 in CAD Patients</b> .....	45
3.3.5.	<b>Decreased expression of Bcl-2 in CAD Patients</b> .....	46

3.3.6.	Upregulated expression of BAX in CAD Patients .....	46
3.3.7.	Increased expression of ET-1 in CAD Patients .....	47
3.4.	Fluorescence-based quantification of miR-1-3p .....	47
3.5.	Evaluation of ISO induced CAD in animal model .....	48
3.5.1.	Assessment of Baseline Characteristics in animal model .....	48
3.5.2.	Oxidative Stress Profiling for Pathological Confirmation .....	48
3.5.2.1.	Assessment of oxidants level in animal model .....	48
3.5.2.2.	Evaluation of antioxidants enzyme activity in animal model .....	49
3.5.3.	Assessment of liver function tests in animal model .....	50
3.5.4.	Evaluation of lipids level in animal model .....	50
3.5.5.	Analysis of mRNA/miRNA expression in animal model .....	51
3.5.5.1.	Increased miR-1-3p expression in ISO induced animal model .....	51
3.5.5.2.	Decreased miR-98-5p expression in ISO induced animal model .....	51
3.5.5.3.	Dysregulated NFATc3 expression in ISO-induced animal model .....	52
3.5.5.4.	Upregulated Et-1 expression in ISO-induced Rat's Tissues .....	52
3.5.5.5.	Downregulated Bcl-2 expression in ISO-induced Rat's Tissues .....	53
3.5.5.6.	Upregulated Bax expression in ISO-induced Rat's Tissues .....	53
3.5.6.	Evaluation of Protein Expression Analysis in ISO induced rat model ..	53
3.5.6.1.	Increased NFATc3 protein expression in ISO group .....	54
3.5.6.2.	Upregulated BAX protein expression in ISO group .....	54
3.5.6.3.	Upregulated Drp-1 protein expression in ISO group .....	55
3.5.6.4.	Upregulated Et-1 protein expression in ISO group .....	55
3.5.7.	Histological investigation of Rat's Heart tissue .....	56
4.	DISCUSSION .....	57
5.	REFERENCES .....	63

**LIST OF ABBREVIATIONS**

<b>AGO</b>	Argonaute
<b>ALT</b>	Alanine Aminotransferase
<b>AMI</b>	Acute Myocardial Infarction
<b>APS</b>	Ammonium Persulphate
<b>APX</b>	Ascorbate Peroxidase
<b>AST</b>	Aspartate Aminotransferase
<b>ATP</b>	Adenosine Triphosphate
<b>BAX</b>	Bcl-2 Associated X
<b>BCIP</b>	5-Bromo-4-Chloro-3-Indolylphosphate
<b>BSA</b>	Bovine Serum Albumin
<b>Ca<sup>+2</sup></b>	Calcium
<b>CAD</b>	Coronary Artery Disease
<b>cAMP</b>	Cyclic Adenosine Monophosphate
<b>CAT</b>	Catalase
<b>CAT</b>	Catalase
<b>CK</b>	Creatine Kinase
<b>CK-MB</b>	Creatine Kinase Myocardial Band
<b>CRP</b>	C-Reactive Protein
<b>cTn</b>	Cardiac Troponin
<b>CVDs</b>	Cardiovascular Diseases
<b>CVDs</b>	Cardiovascular Diseases
<b>cyt c</b>	Cytochrome Complex
<b>DAG</b>	Diacylglycerol
<b>DEPPD</b>	N, N-Diethyl Para-Phenylenediamine
<b>DGSR8</b>	DiGeorge syndrome critical region 8
<b>dNTPs</b>	Deoxynucleotide Triphosphates
<b>DRP-1</b>	Dynamin-related protein
<b>DTNB</b>	5,5'-Dithiobis-2-Nitrobenzoic Acid
<b>ECG</b>	Electrocardiogram
<b>EDTA</b>	Ethylene diamine tetraacetic acid
<b>eNOS</b>	Endothelial nitric oxide synthase

<b>ET-1</b>	Endothelin-1
<b>FeSO<sub>4</sub></b>	Ferrous Sulphate
<b>FP</b>	Forward Primer
<b>G-3-P</b>	Glycerol 3-Phosphate
<b>Gata 4</b>	GATA binding protein 4
<b>GC</b>	Guanylyl cyclase
<b>GK</b>	Glycerol Kinase
<b>GPBB</b>	BB glycogen phosphorylase
<b>GPCR</b>	G-Protein Coupled Receptor
<b>GSH</b>	Glutathione
<b>GSH-Px</b>	Glutathione peroxidase
<b>H&amp;E</b>	Hematoxylin and Eosin
<b>H<sub>2</sub>O<sub>2</sub></b>	Hydrogen Peroxide
<b>h-FABP</b>	Heart-type Fatty acid Binding Protein
<b>ISO</b>	Isoproterenol
<b>LDL</b>	Low density Lipoprotein
<b>M-CSF</b>	Macrophage-Colony Stimulating Factor
<b>MDA</b>	Malondialdehyde
<b>MDH</b>	Malate Dehydrogenase
<b>MDHA</b>	Mono-Dehydroascorbic Acid
<b>Mef2a</b>	Myocyte Enhancer Factor 2a
<b>Mfn-2</b>	Mitofusion-2
<b>MI</b>	Myocardial Infarction
<b>mRNA</b>	Messenger RNA
<b>NaCl</b>	Sodium Chloride
<b>NBT</b>	Nitro-Blue Tetrazolium
<b>NC</b>	Negative Control
<b>NFAT</b>	Nuclear Factor of Activated T cells
<b>NIH</b>	National Institute of Health
<b>NO</b>	Nitric Oxide
<b>NOX4</b>	NADPH Oxidase 4
<b>Ox-LDL</b>	Oxidized LDL

<b>PBS</b>	Phosphate Buffered Saline
<b>PIWI</b>	P-element induced wimpy testes
<b>PMSF</b>	Phenyl Methylsulfonyl Fluoride
<b>pre-miRNA</b>	Precursor miRNA
<b>pri-miRNA</b>	Primary miRNA
<b>Prx</b>	Peroxiredoxin
<b>RIPA</b>	Radio Immune Precipitation Assay
<b>RIPA</b>	Radio Immune Precipitation Assay
<b>RISC</b>	RNA Induced Silencing Complex
<b>RISC</b>	RNA-Induced Silencing Complex
<b>RNA</b>	Ribonucleic acid
<b>ROS</b>	Reactive Oxygen Species
<b>ROS</b>	Reactive Oxygen Species
<b>RP</b>	Reverse Primer
<b>RT-qPCR</b>	Real Time-quantitative Polymerase Chain Reaction
<b>SDS</b>	Sodium Dodecyl Sulfate
<b>SMCs</b>	Smooth muscle cells
<b>SNS</b>	Sympathetic Nervous System
<b>SOD</b>	Superoxide Dismutase
<b>SOD</b>	Super Oxide Dismutase
<b>STEMI</b>	ST Elevation Myocardial Infarction
<b>TBA</b>	Thiobarbituric Acid
<b>TBARs</b>	Thiobarbituric Acid Reactive Substances
<b>TBST</b>	Tris Buffered Saline With 0.1% Tween-20
<b>TCA</b>	Trichloroacetic Acid
<b>TGs</b>	Triglycerides
<b>TNB</b>	5'-Thio-2-Nitrobenzoic Acid
<b>TRBP</b>	Trans Activation Response RNA Binding Protein
<b>US</b>	United States
<b>UTR</b>	Untranslated Region

<b>VSMCs</b>	Vascular Smooth muscle cells
<b>WHO</b>	World Health Organization
<b>XDH</b>	Xanthine Dehydrogenase
<b>XO</b>	Xanthine Oxidase

## LIST OF FIGURES

Figure 1.1 Risk factors causing Oxidative damage to cells and eventually leading to CAD development. ....	2
Figure 1.2 Oxidative Stress Condition.....	3
Figure 1.3 Classification of Antioxidants .....	4
Figure 1.4 Biogenesis and action of miRNA .....	8
Figure 1.5 Development and Progression of Atherosclerosis.....	13
Figure 1.6 Disruption of Cellular Pathways in ISO induced Rat model.....	14
Figure 2.1 Experimental Workflow .....	17
Figure 2.2 Dissection Plan .....	18
Figure 2.3 BSA Standard Curve .....	20
Figure 2.4 Standard Curve for Fluorescence Intensity based Quantification of miRNAs .....	31
Figure 3.3.1 Graphical Representation of Gender-wise Distribution of CAD Patients .....	41
Figure 3.2 Graphical Representation of Age-wise Distribution of CAD Patients .....	42
Figure 3.3 Graphical Representation of other diseases in CAD Patients .....	43
Figure 3.4 Graphical Representation of Smoking Status in CAD Patients.....	43
Figure 3.6 Graphical showing the Fold activity of miR-1-3p in Human Blood sample .....	44
Figure 3.7 Graphical showing the Relative fold activity of miR-98-5p in Human Blood sample .....	45
Figure 3.8 Relative Fold Activity of NFATc3.....	45
Figure 3.9 Relative Fold Activity of Bcl-2 .....	46
Figure 3.10 Relative Fold Activity of BAX.....	46
Figure 3.11 Relative Fold Activity of Et-1 .....	47
Figure 3.12 Fluorescence Intensity based Quantification of miR-1-3p.....	47
Figure 3.13 Baseline Characteristics of Rats .....	48
Figure 3.14 Oxidative Profiling of Rats .....	49
Figure 3.15 Relative activities of Antioxidant Enzyme in Rat's Serum and Heart Tissue Homogenate .....	49
Figure 3.16 Graphical Representation of Liver Function Tests .....	50
Figure 3.17 Graphical Representation of Lipid Profile .....	50



Figure 3.18 Relative fold activity of miR-1-3p in Rat Heart tissue sample .....	51
Figure 3.19 Relative fold activity of miR-98-5p in Rats Blood and Heart Tissues.....	51
Figure 3.20 Relative Fold Activity of NFAT-c3 in Rat's Tissues .....	52
Figure 3.21 Relative Fold Activity of ET-1 in blood and heart tissue of rats.....	52
Figure 3.22 Relative Fold Activity of Bcl-2 in Rat's Tissues .....	53
Figure 3.23 Relative Fold Activity of Bax in Rat's heart tissue .....	53
Figure 3.24 NFATc3 protein expression .....	54
Figure 3.25 BAX protein expression .....	55
Figure 3.26 Drp-1 protein expression level .....	55
Figure 3.27 ET-1 protein expression. ....	56
Figure 3.28 Histological Analysis of Rat's heart tissue.....	56

## LIST OF TABLES

Table 3.1 Gender-wise distribution of CAD Patients .....	41
Table 3.2 Graphical Representation of Age-wise Distribution of CAD Patients .....	42
Table 3.3 Other Diseases in CAD Patients .....	42
Table 3.4 Smoking Status in CAD Patients .....	43

**ABSTRACT**

According to the World Heart Report 2023, 85% of the total cardiovascular diseases associated deaths are caused by coronary artery disease and stroke that is 9.1 million deaths approximately. Coronary artery disease is a complex disorder that involves occlusion of coronary artery, inflammation, and apoptosis of the affected part of the heart. Moreover, there is dysregulation of the microRNAs and their associated target gene signaling pathways. These miRNAs may serve as the diagnostic biomarker for coronary artery disease. This study was aimed to investigate the use of miR-1-3p and miR-98-5p as the potential biomarker for coronary artery disease diagnosis. This study also tried to put forward a novel fluorometric strategy for miRNA quantification. We found an elevated expression of miR-1-3p and decreased expression of miR-98-5p in whole blood samples of coronary artery disease patients. Fluorescence intensity-based quantification of miR-1-3p also showed a remarkably increased quantity of this miRNA in CAD patients. To validate the expression of these miRNAs and their target genes, animal model studies were also conducted. Oxidants and antioxidants biochemical assays confirmed oxidative stress in ISO induced rats. Triglycerides and cholesterol levels were found to be high among the diseased group. Liver markers including activities of AST and ALT were also increased. In the blood and tissue samples of diseased model, Et-1, Bcl-2, and BAX mRNA levels were found to be significantly elevated while NFATc3 mRNA levels were increased in the tissue samples only. To confirm ET-1 as target of miR-98-5p, western blotting was performed after dosing miRNA-98-5p mimics. Upon administration of miRNA-98-5p mimic, Et-1, Drp-1, NFATc3, and BAX protein expression levels were decreased in the diseased group. Furthermore, the histological analysis by H&E staining depicted altered cellular morphology with an elevated percentage of abnormal cells in the diseased group. In conclusion, miR-1-3p and miR-98-5p may serve as potential non-invasive diagnostic biomarkers for coronary artery disease because of their regulatory roles in critical apoptotic and hypertrophic pathways.

## **1. Introduction**

### **1.1. Cardiovascular diseases**

According to a report of World Health Organization (WHO), cardiovascular diseases (CVDs) are an important cause of global deaths. Globally CVDs are known to cause an estimated death of around 17.9 million, annually. According to the statistics given by Centre for Disease Prevention and Control, around 6.9 million people died in 2020 due to heart diseases in United States. Heart diseases comprise of a group of disease conditions involving heart and blood vessels. According to American Heart Association 2023 report, CVD account for 37% of deaths in people of age above 70 (Tsao et al., 2023). Cardiovascular diseases include congenital/rheumatic heart disease, coronary heart disease, thrombosis, cerebrovascular disease, pulmonary embolism and other associated complications. Among these disorders myocardial infarction and stroke account for 85% of the of the CVDs associated deaths.

### **1.2. Myocardial Infarction**

Myocardial infarction (MI) is said to be the acute cardiac event that is initiated by the obstruction of the coronary artery that eventually prevents the blood flow to the portion of heart. This is mostly attributed to the fats' accumulation in the inner walls of coronary blood vessels. It can go undetected in some people, but it can also be a life-threatening event leading to sudden death (Thygesen et al., 2007). Major symptoms of MI are angina pectoris or the chest pain which extends to arm and neck, difficulty in breathing, sweating, nausea, anxiety, fatigue and abnormal heart beat (Kosuge et al., 2006). Various causes for MI include age, smoking, hypertension, increased low-density lipoproteins (LDL), increased body cholesterol and fat levels, physical inactivity, increased body weight, diabetes, chronic kidney disease, high alcohol consumption and sedentary lifestyle (Graham et al., 2007).

### **1.3. Coronary Artery Disease**

Among the several causes of MI, 'coronary artery disease' or 'atherosclerosis' is considered the main cause contributing to 41.2% of total CVD associated deaths in United States (US)(Tsao et al., 2023). Coronary artery disease (CAD) is indicated by defects in the coronary arteries. CAD involves the atherosclerotic coronary arteries that cause ischemia of the heart and eventually result in the Myocardial Infarction (Malakar et al., 2019; Melak & Baynes, 2019). CAD is inflammatory in nature and is manifested

in several forms including angina (either stable or unstable), cardiac death or MI (Álvarez-Álvarez, Zanetti, Carreras-Torres, Moral, & Athanasiadis, 2017).

### 1.3.1. Risk factors

Risk factors for CAD include increased low-density and triglyceride rich lipoprotein cholesterol, physical inactivity, sleep, hypertension, smoking, and lack of exercise, environmental stress, age etc. (Libby, 2021; Pagan et al., 2022). These risk factors are involved in accumulation of ROS in the cardiac cell, eventually leading to oxidative stress. The oxidative stress leads to endothelial dysfunction eventually leading to the atherosclerosis development and MI (Senoner & Dichtl, 2019).

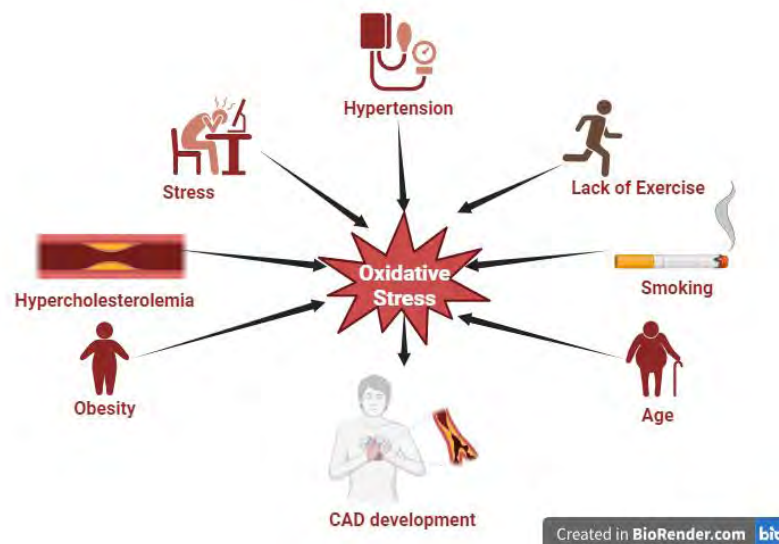


Figure 1.1 Risk factors causing Oxidative damage to cells and eventually leading to CAD development.

### 1.3.2. Oxidative stress

Oxidative stress is the complex biological process that is described as the difference in the reactive oxygen species (ROS) and antioxidants levels in the body. In oxidative stress, increased ROS results in oxidative damage in the cells and other pathological effects in the body. A normal level of ROS is expressed in the cells which is important for many metabolic, and physiological roles (Shankar & Mehendale, 2014). Physiological pathways that involve ROS include redox reactions implicated in protein phosphorylation or dephosphorylation and other metabolic pathways linking carbohydrates, lipid and nucleic acids etc. for homeostatic maintenance (Rotariu et al., 2022). Increase in oxidants in the cells is responsible for cardiovascular diseases. In the development and progression of CAD, oxidative stress remains the key player (Senoner

& Dichtl, 2019). As mentioned earlier different risk factors stimulate atherosclerosis following a different pathway but each of them eventually increases the oxidative stress.

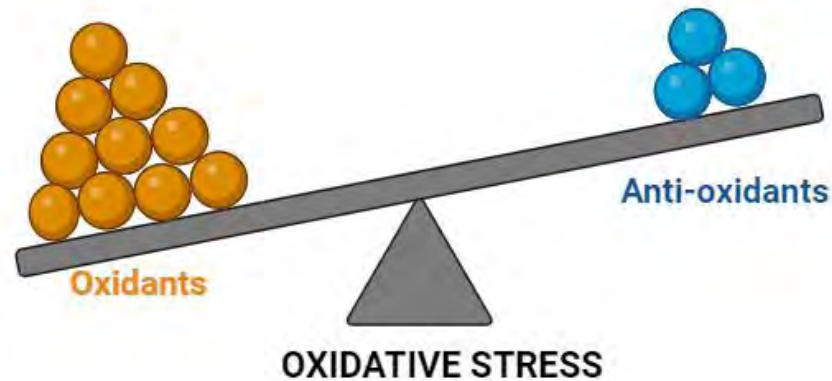


Figure 1.2 Oxidative Stress Condition

### 1.3.3. Sources of ROS in cardiac cells

ROS is broadly classified into two classes; one including oxygen free radicals like superoxide, peroxy radicals, the second class constitute of non-radicals like hydrogen peroxide, hypochlorous acid etc. (Liochev, 2013). There may be multiple sources of ROS in cardiac cells including mitochondria, nitric oxide synthase, NADPH oxidases, Xanthine oxidoreductase, cytochrome P450, monoamine oxidase. Leakage of electrons from the electron transport chain complexes, and the mitochondrial proteins like monoamine oxidase, NADPH Oxidase-4 (NOX-4) are responsible for mitochondrial ROS (Murphy & Liu, 2022). In addition to these sources some other enzymatic reactions are held responsible for ROS synthesis that involved phagocytosis, oxidative phosphorylation and prostaglandin production (Fialkow, Wang, & Downey, 2007).

### 1.3.4. Types of ROS in cardiac cells

Various types of ROS are involved in CVDs development and progression that include superoxide radical and hydrogen peroxide etc. Superoxide radicals are involved in the synthesis of other ROS species like  $H_2O_2$  and  $OH^\cdot$ . They form peroxynitrite ( $ONOO^\cdot$ ) by reacting with the nitric oxide (Pacher, Beckman, & Liaudet, 2007).  $OH^\cdot$  is also generated by the electron exchange reaction between  $O_2^\cdot$  and  $H_2O_2$  (Tsutsui, Kinugawa, & Matsushima, 2011).

### 1.3.5. Antioxidant defense system

Many antioxidant enzymes are present in our body that work to counter the effects of ROS. Antioxidants sometime scavenge ROS, or they may convert ROS into other non-toxic compounds. Antioxidants are of two types: non-enzymatic and enzymatic. The enzymatic antioxidants in our body comprise Superoxide dismutase (SOD), catalase (CAT), peroxiredoxin (Prx), and Glutathione peroxidase (GSH-Px) etc. The non-enzymatic antioxidants comprise glutathione (GSH), ascorbate, beta-carotene, vitamin-E etc. (He et al., 2017; Tan et al., 2023). In normal cellular conditions, these antioxidants are in balance with the oxidants produced by the cells hence nullifying the effects of ROS by their ROS scavenging activity.

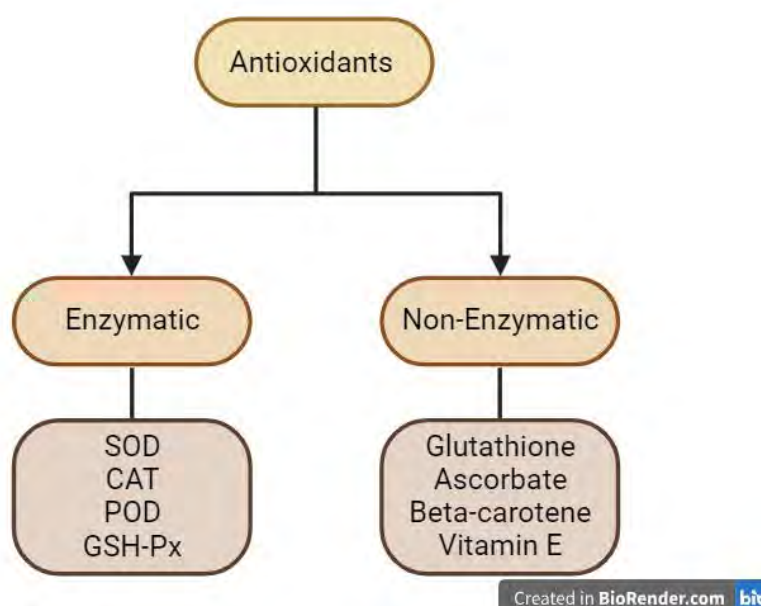


Figure 1.3 Classification of Antioxidants

### 1.4. Major events in CAD development

An imbalance between oxidants and antioxidants in the cardiac cells is responsible for various cardiovascular diseases as they promote endothelial dysfunction and lipid peroxidation as the primary events in CAD development. Moreover, miRNA expression is also dysregulated in response to oxidative stress.

#### *Endothelial dysfunction*

Endothelial nitric oxide synthase (e-NOS) produces nitric oxide (NO) which maintains the arterial endothelium and is also used by all types of blood vessels for dilation by

stimulation of guanylyl cyclase (GC) and increased cGMP in the smooth muscle cells (SMCs) (U Förstermann et al., 1994; Ulrich Förstermann & Münzel, 2006). NO<sup>-</sup> is responsible for inhibiting the leukocyte and platelet aggregation within the endothelium as well as it inhibits mitogenesis and vascular smooth muscle cells (VSMCs) proliferation. Due to these functions, it inhibits the development of atherosclerosis (Ulrich Förstermann & Münzel, 2006; Tibaut & Petrovič, 2016). NO also inhibits the endothelial apoptosis, adhesion molecules' transcription thus stops the leukocytes infiltration in walls of blood vessels (Tibaut & Petrovič, 2016). Increased ROS promotes the conversion of NO in to peroxynitrite (ONOO<sup>-</sup>). This ONOO<sup>-</sup> hence affects the normal functioning of the endothelium leading to endothelial dysfunction (Tibaut & Petrovič, 2016). Oxidative stress also disturbs the cGMP signaling within the vascular cells (Daiber et al., 2021).

### ***Lipid peroxidation***

Oxidative stress is also involved in the lipid peroxidation within the cardiac cells. Cellular ROS including HO<sup>-</sup> and HOO<sup>-</sup> are main causes of lipid oxidation. Lipid peroxidation proceeds in a “chain reaction mechanism” that involves initiation, propagation, and termination. First, the free radical is produced by the loss of hydrogen from unsaturated lipid molecules. The lipid radical and oxygen react forming the peroxy radical in the propagation step. This peroxy radical then attacks other lipids to make more peroxy radicals (Gianazza, Brioschi, Fernandez, & Banfi, 2019; Tsikas, 2017). Low-density lipoprotein (LDL) oxidation is also stimulated by oxidative stress which has several effects on development and progression of CAD. Endothelial dysfunction caused due to disruption of NO by oxidative stress results in the movement of plasma LDL into the arterial wall. This LDL is then oxidized forming oxidized LDL (Ox-LDL) (Wang & Kang, 2020). Ox-LDL has multiple consequences including increased endothelial injury, increased inflammatory cell adhesion to macrophages as well as their differentiation, enhanced aggregation of platelets, enhanced inhibition of eNOS, and increased inflammatory cytokine release (Gianazza et al., 2019).

### ***Dysregulated miRNA expression***

Numerous studies associate the development of several cardiovascular diseases with the disturbed expression of non-coding RNAs. Micro-RNAs are a highly conserved



class of non-coding RNAs. They are responsible for regulating the post-transcriptional expression of several genes. Several roles of mi-RNA have been studied that include gene silencing, mRNA degradation or translation inhibition and blocking. In cardiovascular diseases, oxidative stress dysregulates miRNAs involved in regulating multiple cellular pathways hence promoting CAD development (L. F. Gebert & I. J. MacRae, 2019; Xu et al., 2021).

### **1.5. Biogenesis of miRNA**

miRNA biogenesis is a multi-stage process that requires multiple proteins and cellular locations.

#### ***Primary-miRNA transcription***

miRNA biogenesis is initiated with the generation of the primary miRNA transcripts (pri-miRNA). This step requires RNA polymerase II. These pri-miRNA are synthesized either by specific miRNA gene or miRNA clusters or introns of the coding genes called mono-cistronic or intronic respectively (Acuña, Floeter-Winter, & Muxel, 2020; Leitão & Enguita, 2022).

#### ***Precursor-miRNA synthesis***

Microprocessor complex acts upon the pri-miRNA and process them into the hair-pin structured RNA now termed as the precursor miRNA (pre-miRNA). This step occurs within the nucleus. Drosha or microprocessor complex is comprised of double stranded RNA binding protein, Drosha, RNase III, DiGeorge syndrome critical region 8 (DGCR8) and many other proteins. (Ha & Kim, 2014; Leitão & Enguita, 2022).

#### ***Export of pre-miRNA to cytoplasm***

After the processing of pre-miRNA, it is moved out from the nucleus to the cytoplasm. This export is mediated by protein exportin-5 which first forms a complex with the RAN.GTP. RAN.GTP is a GTP-binding nuclear protein. The GTP bound with the protein gets hydrolyzed after the export that results in the disassembly of complex and pre-miRNA is released in the cytosol (Ha & Kim, 2014).

#### ***Cytoplasmic processing of pre-miRNA***

The pre-miRNA is acted upon by the cytoplasmic Dicer that is RNase III type endonuclease. It cleaves the pre-miRNA from its terminal loop and liberate a 21-24 nucleotide long duplex of miRNA (Ha & Kim, 2014; H. Zhang, Kolb, Jaskiewicz, Westhof, & Filipowicz, 2004).

### ***RISC complex Assembly***

RNA induced silencing complex (RISC) formation is done by loading newly formed miRNA duplex on the argonaute protein (Ago). AGO consists of a single polypeptide chain having four domains; amino domain at N-terminal, middle (MID) domain, the P element induced wimpy testes domain (PIWI) and the PAZ domain (Piwi-Argonaute-Zwille). The miRNA's 5' end is held between MID and PIWI domains whereas the PAZ domain hold 3' end of miRNA (Treiber, Treiber, & Meister, 2019). The mammalian genome encode four Ago proteins but only Ago2 protein possess the slicer activity required for gene silencing (Park et al., 2017).

### ***miRNA strand cleavage***

After the RISC assembly, one miRNA strand of the loaded duplex miRNA is cleaved. The strand that is cleaved is called the 'passenger' strand while the retained strand is named as 'guide' strand. The 'guide' strand remains associated to the Ago proteins and RISC. This completes RISC assembly and stabilizes it (L. F. R. Gebert & I. J. MacRae, 2019; Ha & Kim, 2014; Matsuyama & Suzuki, 2020; Treiber et al., 2019).

## **1.6. Action of miRNA**

The miRNA mediated gene expression regulations involve miRNA target sites in the target mRNA. The miRNAs target those sequences in 3' UTR of the target mRNAs which are complementary to their 'seed sequences'. Initial miRNA and mRNA binding is done using the MID and PIWI domains of the Ago proteins and is mediated by complementary initial nucleotides. This binding is retained if high sequence complementarity is present between the seed sequence and target mRNA. The complementarity of target site to the 2-7 or 3-8 nucleotide is considered canonical. When the Ago-miRNA binds to the 3' UTR of target mRNA it can mediate silencing either by mRNA decay or the translational repression (Leitão & Enguita, 2022).

The miRNA can regulate gene expression by translational inhibition mRNAs having 5' 7-methylguanosine cap. When the miRNA binds these mRNA, it inhibits the binding of initiation factors of translation including eIF4E, eIF4F and eIF4G. This promotes target mRNA scaffolding and hence association of ribosome initiation complex (Naeli, Winter, Hackett, Alboushi, & Jafarnejad). AGO2-Dicer-TRBP complex can also prevent the association of ribosomal subunits and mRNA (Acuña et al., 2020).

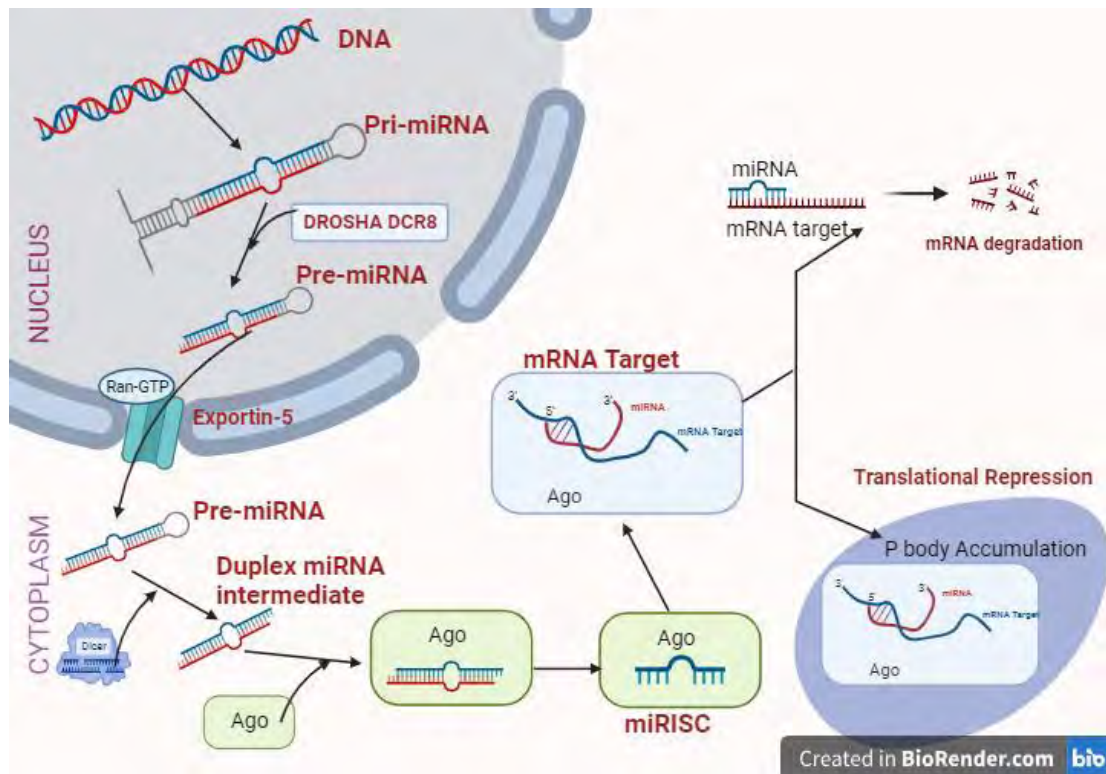


Figure 1.4 Biogenesis and action of miRNA

### 1.6.1. Dysregulated miRNAs in CAD

Several miRNAs are involved in CAD development and progress by dysregulating the expression of various genes and disturbing their normal physiological roles. As certain miRNAs have dysregulated expression in the disease conditions, they can be considered as the potential biomarker for a particular disease. Under disease circumstances, certain miRNAs have dysregulated expression that results in dysregulated expression of their target genes. The deregulated gene expression thus results in the progression of the disease. miRNA-1-3p and miRNA-98a-5p are the potential miRNAs involved in CAD and eventually in the MI.

The miR-1 is found to be cardiac-specific and has shown different regulatory roles. It modulates the differentiation and proliferation during cardiogenesis and the growth of cardiomyocytes in adult heart. miR-1 also inhibits cardiac hypertrophy (Badacz et al., 2021; Navickas et al., 2016). miR-1 inhibits the CaN/NFAT signaling pathway in the cardiomyocytes by downregulating the NFAT (nuclear factor of activated T cells), Mef2a (myocyte enhancer factor 2a) and GATA binding protein 4 (Gata 4) thus negatively regulates the cardiomyocyte hypertrophy. It also mediates MAPK pathway and hence promote angiogenesis by inhibiting Spred-1 (Gholaminejad et al., 2021).

miR-98a-5p is studied to be involved in the ROS related apoptosis of cardiomyocytes (Sun et al., 2017). miR-98a-5p also has roles in cellular viability by targeting LOX-1 (Ali Sheikh et al., 2021; Sheikh, 2020). This miRNA also targets *ET-1* (endothelin-1) and thus mediates the endothelial cells' proliferation (Kang et al., 2016).

Upregulation of miRNA can downregulate its target genes in CAD. Dysfunction of various genes is involved in the progression of the CAD, including the genes involved in apoptotic signaling pathways of either the VSMCs as well as the other cells involved in atherosclerosis lesion like ET-1, Bcl-2, BAX, Drp-1 and NFAT-c3.

### **1.6.2. Target genes**

Depending on the dysregulated expression of the miRNAs, the target genes' expression is affected. In the case of CAD, various genes related to apoptosis, cellular differentiation, lipid transport, endothelial dysfunction etc. are dysregulated that eventually favors the development and progression of pathological condition.

#### ***NFATc3***

The transcription factor family of NFAT was first identified in the T cells. NFAT was found to be activated by the antigen receptors that are coupled with the mobilization of calcium. NFAT is present initially in the cytoplasm and after receiving the calcium signal, it is translocated to the nucleus. For its transport into the nucleus, calcineurin (which is a calcium-calmodulin dependent phosphatase) dephosphorylates NFAT. Once in the nucleus, NFAT mediates the transcription of the cytokines in many cells that include T lymphocytes, fibroblasts, endothelial or macrophage (Cai et al., 2021; Harada et al., 2014). In macrophages, NFATc3 is involved in the expression of miR-204. miR-204-5p downregulates the expression of scavenger receptor-A(SR-A) while miR-204-

3p downregulates CD36 receptors in macrophages (Liu et al., 2021). The function of SR-A is to uptake modified lipoproteins and promote the accumulation of cholesterol in arterial walls. CD36 has roles in foam cell formation, macrophage migration, activation of inflammasome, endothelial apoptosis and thrombosis (Zhao, Varghese, Moorhead, Chen, & Ruan, 2018).

### ***Bcl-2***

Bcl-2 family members include 20 anti- and pro-apoptotic proteins that regulate mitochondrial apoptotic pathway. Bcl-2 protein is an anti-apoptotic protein that prevents apoptosis without affecting cellular proliferation (Su, Sun, Liu, Shu, & Liang, 2018). This protein family is a major player in the apoptosis system regulating mitochondrial membrane permeability. This protein family members are involved also in various other cellular mechanisms (Warren, Wong-Brown, & Bowden, 2019). These family proteins are classified as either pro-apoptotic BAX, Bak, etc. or anti-apoptotic Bcl-2 protein. Increase in BAX/Bcl-2 ratio promotes cellular apoptosis. According to a study it was observed that decreasing the microRNA-34a levels facilitate endothelial cells growth and inhibited apoptosis in an atherosclerotic plaque (AP) by activation of the anti-apoptotic Bcl-2 protein. This result suggested a promising therapeutic possibility for atherosclerosis. APs contain a huge quantity of dead cells that makes up to 80% of the total structure of AP (T. Zhang et al., 2015).

### ***ET-1***

Endothelin-1 (ET-1) is a peptide that regulates endothelial dysfunction. Its primary roles include vasoconstriction and inflammation. Physiologically, ET-1 production is reduced in endothelial cells, but its expression is increased in the pathophysiological conditions in many cells including VSMCs, cardiac myocytes, endothelial cells, macrophages, and leukocytes. ET-1 also decreases the expression of eNOS hence reduces the NO synthesis. This eventually promotes the vascular dysfunction (Böhm & Pernow, 2007; Muniyappa, Chen, Montagnani, Sherman, & Quon, 2020).

### ***BAX (Bcl-2 Associated X) Protein***

BAX is an outer-mitochondrial membrane protein that is involved in regulating cellular apoptosis. It is a member of the Bcl-2 protein family and has a pro-apoptotic role in atherosclerosis (Zhou et al., 2023). Its activation by Bcl-2 protein, in response to

oxidative stress, increases the membrane permeability of mitochondria releasing cytochrome c into the cytosol (Wolf, Schoeniger, & Edlich, 2022). Apoptosis of macrophages, SMCs (smooth muscle cells), and ECs contribute to progression of arterial atherosclerosis (Warren et al., 2019).

### ***Drp-1***

During apoptosis, mitochondrial fission has been reported to occur. The equilibrium between mitochondrial fission and fusion is maintained by various proteins. Dynamin-related protein (Drp-1) is the protein known to be involved in mitochondrial fission process (Karbowski et al., 2002). Drp-1 along-with BAX mediates the mitochondrial membrane integrity (Chiong et al., 2011). Decreased mitofusion-2 (MFN-2) protein an increased Drp-1 and BAX causes the mitochondrial fragmentation and cytochrome c release, hence causing apoptosis (Parra et al., 2008).

## **1.7. Stages of CAD development**

Development of CAD can be divided into multiple events that occur during atherosclerotic progression from oxidative stress till thrombosis eventually leading to myocardial infarction. The normal arterial wall has three layers namely, tunica intima, tunica media and tunica adventitia. Tunica intima is composed of monolayer ECs while tunica media is composed of SMCs. Different events are mentioned below.

### ***Endothelial dysfunction and lipid accumulation***

CAD begins with endothelial dysfunction caused due to oxidative stress. In physiological conditions, endothelial derived NO is responsible for maintenance of the endothelial integrity (Incalza et al., 2018). As the endothelium becomes dysfunctional, it turns 'leaky' at the cellular junctions and there is an accumulation of the LDL in the intima of the vessel (X. Zhang, Sessa, & Fernández-Hernando, 2018). These LDL molecules are then oxidized because of the oxidative stress which further stimulates the activation of endothelial layer. The activated endothelial layer has increased expression of chemotactic and adhesion molecules on its surface resulting in increased uptake of LDL molecules. This oxidation of the LDL also triggers the inflammation in the region (Mundi et al., 2017).

### ***Uptake of Monocytes and differentiation***

As the chemotactic and adhesion molecules including VCAM, ICAM1, P-selectin, E-selectin are expressed on the surface of the endothelium, they promote the adhesion and subsequent uptake of the monocytes by the vessel's endothelial cells (Medina-Leyte et al., 2021). Once entered, they are differentiated into macrophages and begin secreting macrophage-colony stimulating factor (M-CSF) (Björkegren & Lusis, 2022; Tabas & Bornfeldt, 2020).

### ***Formation of foam cells***

The differentiated monocytes (now called macrophages) also uptake the modified lipoproteins and become foam cells. The unmodified form of lipids cannot be engulfed by macrophages so lipids must be first modified or aggregated. Using the scavenger receptors on the surface of the macrophages or via phagocytosis, modified lipids are engulfed and foam cells are formed (Björkegren & Lusis, 2022; Tabas & Bornfeldt, 2020).

### ***Formation of necrotic core***

These foam cells mostly undergo necrosis or apoptosis and promote the formation of the necrotic core. This necrotic core also contains cholesterol esters, cholesterol crystals and cellular debris. All of these eventually help in promoting the lesion rupture (Björkegren & Lusis, 2022).

### ***Atherosclerotic lesions***

Not only macrophages but the smooth muscle cells from the 'medial layer' start migrating into the 'intimal layer'. Once in the intima, they also transform into macrophage-like foam cells and stimulate the collagen deposition forming 'fibrous cap' in the growing necrotic core. B and T cells also enter into the lesion and promote lesion growth (Basatemur, Jørgensen, Clarke, Bennett, & Mallat, 2019).

### ***Thrombosis***

As the necrotic core has cholesterol and cholesterol esters content, the cells in the core die frequently. This is also coupled with the calcium deposition in intima or media layer of the vessel. Calcification is actually initiated and promoted by the apoptosis of the macrophages as well as the SMCs (Mori et al., 2018). Macrophages and neutrophils are

the main drivers for plaque instability. Plaque instability eventually leads to the endothelial erosion leading to thrombosis and eventually resulting MI (Gonzalez & Trigatti, 2017; Martinet, Schrijvers, & De Meyer, 2011).

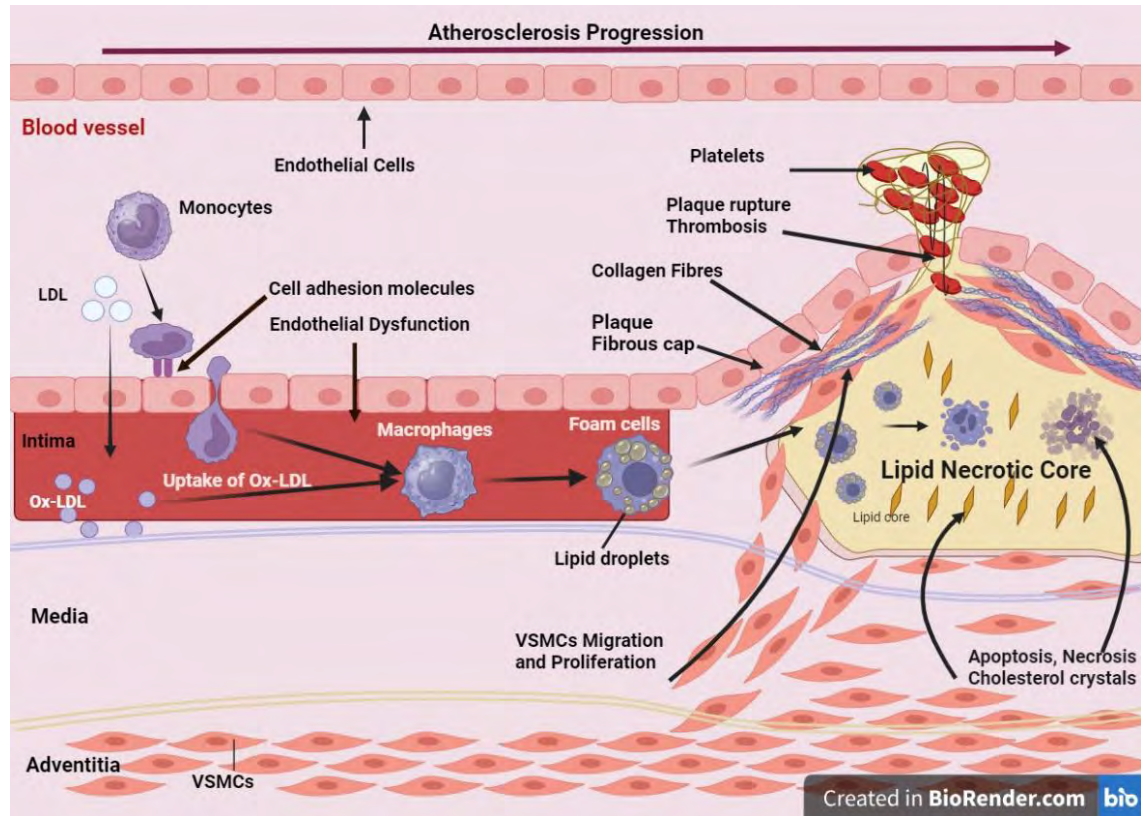


Figure 1.5 Development and Progression of Atherosclerosis

### 1.8. ISO induced CAD leading to MI in rat model

Isoproterenol (ISO) is a synthetic agonist of  $\beta$ -adrenergic receptors or  $\beta$ -adrenoceptors (Rajadurai & Stanely Mainzen Prince, 2007). It has been reported to induce MI at doses ranging from 85 to 340 mg per kg in rats. It is known to develop oxidative stress by raising free radicals and declining the anti-oxidative defense mechanisms (Mohan Manu, Anand, Sharath Babu, Patil, & Khanum, 2022). ISO dose also leads to apoptosis, hypoxia and other cardiotoxic events (Lobo Filho et al., 2011). The cardiotoxic conditions caused as a result of ISO induction in rats is similar to human MI and hence makes it a suitable model for MI studies (Hosseini et al., 2022).



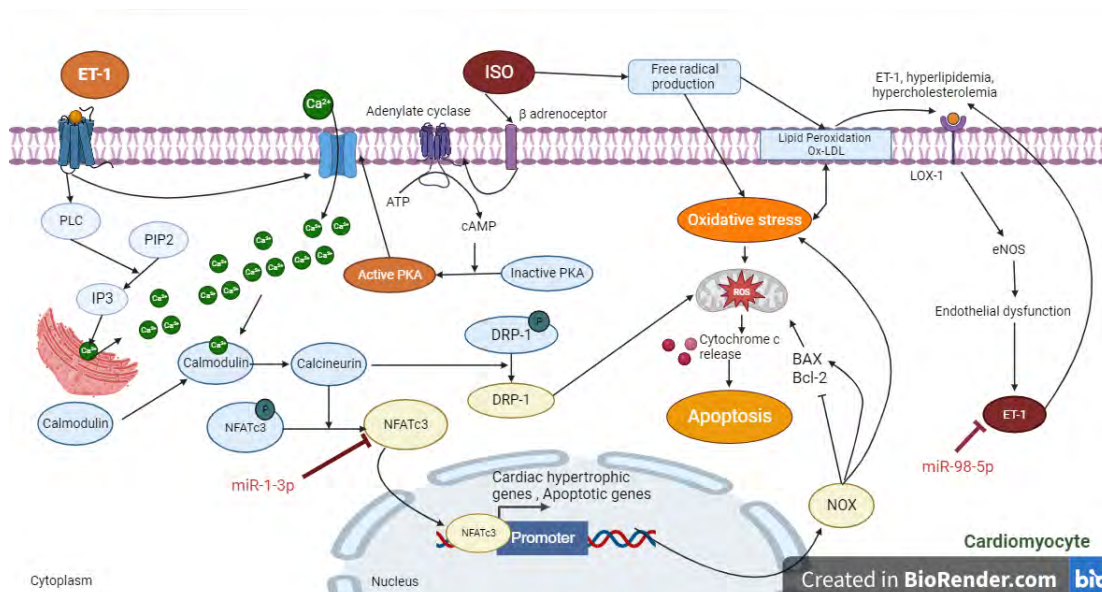


Figure 1.6 Disruption of Cellular Pathways in ISO induced Rat model

## 1.9. Diagnosis of CAD

CAD leads to MI, which can be life threatening, if not diagnosed and treated on time. Earlier diagnosis of CAD provides better opportunity for the treatment of MI. For diagnosis of MI, several strategies and biomarkers are used. These biomarkers include cardiac troponins, plasma myoglobin levels, the catalytic activity of total creatine kinase (CK), heart-type fatty acid binding protein (hFABP), isozyme BB glycogen phosphorylase (GPBB) and Copeptin (Janota, 2014). Out of these biomarkers, cardiac troponin levels were considered as a gold-standard for MI diagnosis, but it is found to be elevated also in case of end stage renal disease. The levels of cardiac troponins are also related to time-change (Solaro & Solaro, 2020). So, it is proposed that these biomarkers can be a prognostic marker rather than diagnostic biomarker MI (Ellis et al., 2022; L. M. Li et al., 2014).

miRNAs are considered as an early cardiac biomarker. They are comparatively more sensitive and specific biomarkers for cardiovascular diseases. Cardiac cells express and release specific miRNAs in the blood stream and their levels increase significantly in response to ischemia or cardiac damage (Ellis et al., 2022). miRNA levels are elevated in blood earlier than the cardiac troponins and hence they can be an earlier diagnostic biomarker for CAD leading to MI (X. Chen et al., 2015).

### **1.10. Aims And Objectives**

The aim of this study is to design a diagnostic panel for early detection of CAD associated MI.

The objectives of this study include:

- Assessment of selected miRNAs as the diagnostic biomarker for CAD detection in patients' samples
- Validation of miRNAs and their target genes expression in animal model
- Confirmation of miRNA target genes by administering miRNA mimic

#### **Disclaimer:**

The data in this thesis is confidential and under patent review.

## **2. MATERIALS AND METHODS**

### **2.1. Study Hypothesis**

This study was conducted to assess the role of RNA interference in the progression of CAD leading to MI. miRNAs can play a very crucial role in the CAD development by regulating the expression of many genes like Drp-1, NFATc3 and Bcl-2, BAX etc. involved in apoptotic signaling pathways. The progression of CAD can eventually lead to MI. Therefore, these miRNAs can potentially help in the early diagnosis of MI. The purpose of this study was to investigate the diagnostic potential of miRNA-1-3p and miR-98a-5p along with their putative targeted genes including NFATc3, and ET-1, and to investigate the disrupted apoptotic signaling in CAD. The detection of CAD can help in the earlier treatment thus reducing the risk of myocardial infarction associated with CAD. The objective of this study was to design a diagnostic panel for earlier CAD detection using miRNAs and elucidate their putative target genes' expression.

### **2.2. Study Design**

To study the role of miRNAs and their putative downstream apoptotic signaling markers, blood samples from both humans and rats while heart tissue samples from rats were taken. For this study, Sprague Dawley rats were separated in seven groups including Normal, Isoproterenol (ISO), ISO+ miR-98a-5p mimic, miR-98a-5p mimic, ISO+ negative control (NC), NC, and vehicle. RNA extraction was done from both human and rat samples, followed by cDNA library synthesis and qRT-PCR for evaluating the expression of various miRNAs and their potential target genes. Serum and heart tissue homogenates samples of rats were used for biochemical analysis including oxidants, antioxidants, lipid, and liver function profiles. Western Blotting was performed to assess the expression of various apoptotic genes potentially associated with CAD and for target genes confirmation of miR-98a-5p.

### **2.3. Ethical considerations**

After the ethical approval from the Ethical Committee, Quaid-i-Azam University, Islamabad, the study was conducted on both human and rat samples. All the experimentation was done in accordance with the Declaration of Helsinki USA and National Institute of Health (NIH), Islamabad, Pakistan. Sprague Dawley rats were kept

in the Primate Facility of Quaid-i-Azam University where they were provided with adequate feed and water supply.

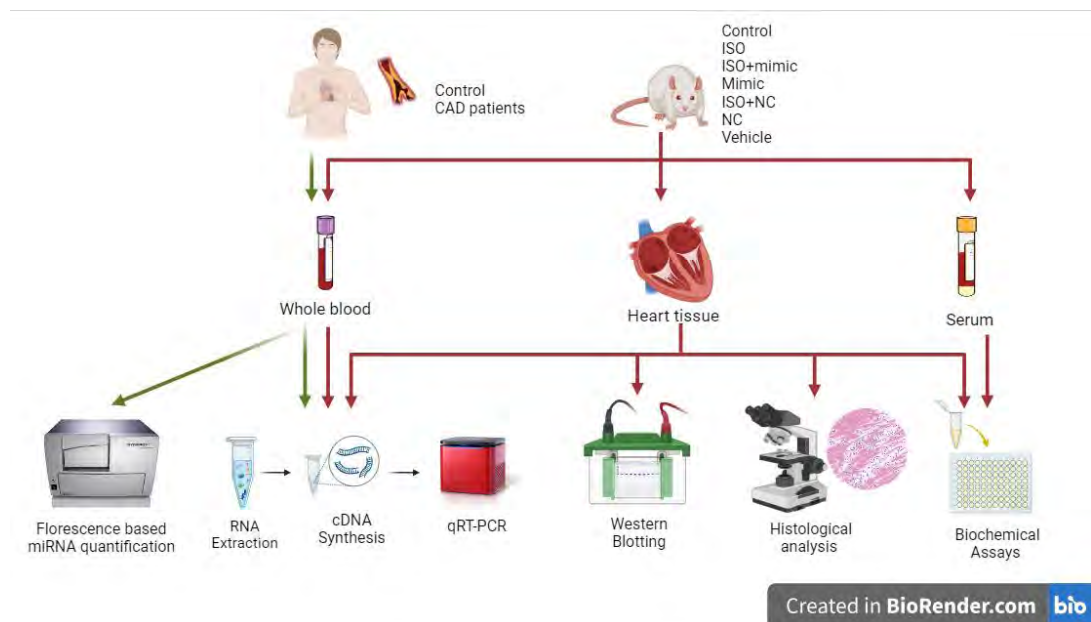


Figure 2.1 Experimental Workflow

## 2.4. Sample collection

Human blood samples were collected from the Armed Forces Institute of Cardiology, Military Hospital, Rawalpindi. In the control group, individuals with <math><50\%</math> coronary artery stenosis were included. For the disease group, individuals with  $\geq 50\%$  coronary artery stenosis, and Myocardial Infarction confirmed by angiography were included in the study after informed consent. The blood samples were saved in EDTA tubes. Afterwards, the blood was transferred to Eppendorf tubes and RNA Later was added to it. RNA later fixes the blood and degrades nucleases in the sample. The samples were then stored at  $-80^{\circ}\text{C}$  until further processing.

## 2.5. Dose regimen and sample collection from Sprague Dawley Rats

For conducting the experimental studies, rats of body weight 110-180 g were chosen. The rats were separated into groups including normal, diseased, and mimic administered. Rats in the normal control group received 500ul of normal saline for 14 alternative days. Diseased rats were given 5mg/kg body weight isoproterenol subcutaneously for 14 consecutive days. Rats in the mimic administered group were

given 2nmol of miR-98-5p mimic using atelocollagen as vehicle making a total volume of 200 ul along with ISO dose.

After completion of the dosing period, the rats were weighed and dissected. Blood and organ samples were collected from the rats. The blood was collected in the serum tubes. The heart was weighed and divided into five fractions, two for homogenate preparation and RNA extraction each and one for histological staining. For RNA extraction, the samples were treated with 350 µl Trizol Reagent. For homogenate preparation, the fractions were treated with 200 µl extraction buffer. Both samples were saved at -80°C until further processing. For histological investigation, a section of heart were preserved in 10% formalin solution.

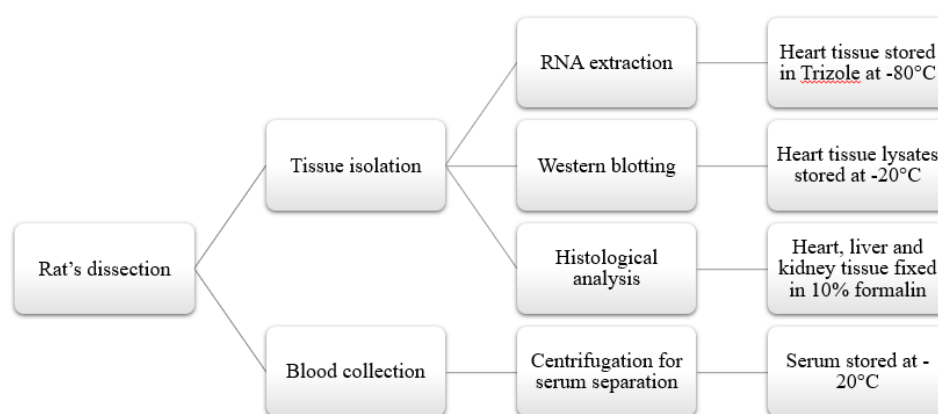


Figure 2.2 Dissection Plan

## 2.6. Tissue homogenization

For the biochemical analysis, heart tissue was homogenized by the following procedure (Ishtiaq et al., 2020).

### 2.6.1. Lysis buffer

For preparing the tissue lysates, Radio-immunoprecipitation assay (RIPA) lysis buffer was prepared using following recipe.

Reagents	Concentration

Tris -HCl	10mM (at pH 8.0)
EDTA (Ethylenediamine Tetra Acetic Acid)	1mM
Triton X-100	1ml
SDS	0.1%
Sodium Chloride (NaCl)	140mM
Sodium deoxy cholate	0.1%
Phenyl MethylSulfonylFluoride (PMSF)	25mg/ml

Out of the heart tissue fractions stored for homogenate preparation, 100 mg of the heart tissue was weighed. 150 $\mu$ l lysis buffer containing PMSF is added in the tissue. The tissue is first minced using the surgical blades and finally homogenized using electric homogenizer. After homogenizing the samples, centrifugation was done at 13000rpm for 10 minutes. The supernatant was taken and stored at -20°C. These homogenates will then be used for biochemical assays.

## 2.7. Protein Quantification using Bradford Assay

For quantifying the proteins present in the homogenates, Bradford Assay was performed. In order to generate a standard BSA curve, serial dilutions (5M-10M) of BSA were prepared and absorbance reading was recorded at 595nm by Multiskan Go Microplate spectrophotometer. Reagents required for Bradford Assay are:

Reagents	Concentration
BSA serial dilutions	5-10 M
Distilled Water	
Bradford Reagent	

### Procedure

To make the working Bradford reagent, distilled water and Bradford Reagent was taken in ratio of 1:4. The calculations were done according to the number of samples and BSA dilutions, each in duplicate. Stock of Bradford working solution was prepared first. After that, 10 $\mu$ l of each dilution and sample is poured in separate wells of a microtiter plate. This is followed adding 190  $\mu$ l of Bradford working solution in each well making a ratio of 1:9. 30 minutes incubation at room temperature was done and then the absorbance was recorded at 595nm by Multiskan GO spectrophotometer (Thermo fisher Scientific USA). Standard BSA curve was generated, and proteins are quantified using linear line equation.

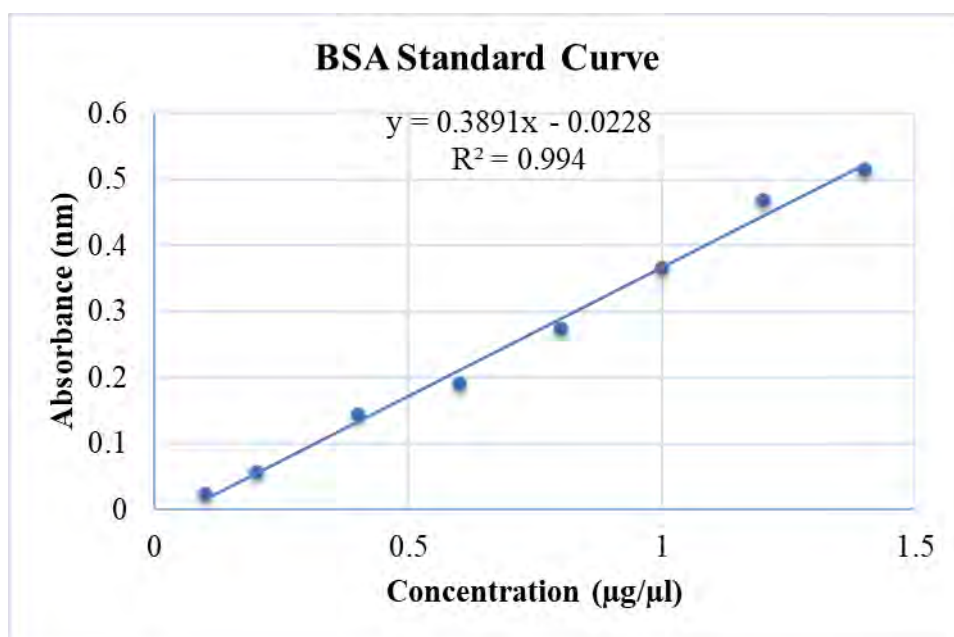


Figure 2.3 BSA Standard Curve

## 2.8. Western Blotting

Western blotting was done to analyze the protein expression in various experimental groups and for confirming the targets of miR-98-5p. Using the western blotting apparatus of Bio-Rad USA, it was done by following the Ma(2006) protocol.

Following are the steps involved in western blotting analysis:

- Preparation of the gel
- Sample preparation and electrophoretic separation of the proteins
- Blocking
- Antibody treatment

- Chromogenic detection
- Preparation of the gel

### 2.8.1. Preparation of the gel

#### Reagents

Reagents	Separating gel (10%)	Stacking gel (4%)
Distilled Water	4ml	3500 $\mu$ l
Tris- HCl	2500 $\mu$ l (1.5M at pH 8.8)	625 $\mu$ l (1M at pH 6.8)
10% SDS	0.1ml	50 $\mu$ l
Acr-Bis (30%)	3.3 ml	0.825 ml
APS (10%)	0.1ml	50 $\mu$ l
TEMED	6 $\mu$ l	6 $\mu$ l

#### Procedure

After assembling the gel casting apparatus, 10% separating gel was prepared and poured into the gel casting tray followed by pouring isopropanol on to the gel's surface for removing bubbles. This gel was then allowed to solidify after which the isopropanol was discarded, and the upper surface was rinsed using distilled water and dried properly using filter paper. Afterwards, stacking gel (4%) was made and loaded on the top of separating gel and the comb is placed cautiously for creating wells. This gel is allowed to polymerize and solidify.

### 2.8.2. Sample preparation and electrophoretic separation of the proteins

For preparation of the sample the following reagents were used.

#### 2X SDS- Gel Loading Buffer (100 ml) Reagents

Reagents	Concentration



Glycerol	0.2%
Dithiothreitol	200mM
Tris HCl	62.5 mM at pH 6.8
Bromophenol blue	0.01%
Sodium dodecyl sulfate	2%

### Procedure

Extraction buffer, SDS loading dye and samples were mixed to make up final volume of 15  $\mu$ l. Afterwards, sample incubation was done at 95°C for 10 minutes in a water bath. The samples are then centrifuged for 1 min at 2000rpm.

### 2.8.3. Sample Loading and Gel Running

#### 5X SDS Running Buffer (1000 ml) recipe

Reagents	Concentration
Tris	125mM
SDS	0.50%
Glycine	1.25M

800ml distilled water was added in 2ml 5X SDS Running Buffer to make 1000ml 1X SDS running Buffer.

### Procedure

Using a clamping apparatus, two gel plates were clamped and placed in the gel tank. 1X SDS gel running buffer was poured in gel tank. The comb was removed from the plates followed by sample loading in wells. A known protein marker (protein ladder) was loaded in the first gel. Electrophoresis was first started at 90V until the loading dye reached the separating gel. The voltage was increased to 120V until the samples are

fully resolved. For confirming protein expression, the gel was first stained using Coomassie R-250 using following reagents.

#### 2.8.4. Gel Staining

##### Reagents

##### Fixing Solution

Reagents	Concentration
Distilled water	
Glacial acetic acid	10 %
Methanol	50 %

##### Staining Solution

Reagents	Concentration
Distilled water	
Methanol	50 %
Coomassie R-250	0.1 %
Glacial acetic acid	10%

##### Destaining Solution

Reagents	Concentration (%)
Distilled water	
Methanol	40 %
Glacial acetic acid	10%

##### Storage Solution

5% glacial acetic acid

### Procedure

For staining the gel, it was first removed cautiously from gel plates and placed in fixing solution overnight. Next day, the solution was discarded, and staining solution was poured on the gel and left for 20 minutes. After that, staining solution was removed, and de-staining solution was poured in the gel. This solution was refilled various times until full destaining of gel background and protein bands were observed. Gels that were to be transferred on to nitrocellulose membrane were not stained.

### 2.8.5. Transfer of Proteins on Nitrocellulose Membrane

#### Reagents

Following reagents were required for transfer of proteins on nitrocellulose membrane.

#### Transfer Buffer

Reagents	Concentration
Distilled Water	
Methanol	20 %, 200 ml
Glycine	14.04 g(192mM)
Tris	25 mM

#### Phosphate Buffer Saline (pH 7.4)

Reagents	Concentration
Potassium chloride (KCl)	2.7mM
Sodium Chloride (NaCl)	150mM
Potassium dihydrogen phosphate (KH <sub>2</sub> PO <sub>4</sub> )	1.8 mM

Di sodium hydrogen phosphate (Na <sub>2</sub> HPO <sub>4</sub> )	10.1 mM
Distilled Water	

**Ponceau Stain**

Reagents	Concentration
Distilled water	
Glacial acetic acid	5 ml
Ponceau stain	0.5 g

**Phosphate Buffer Saline (1 L, pH 7.4)**

100 µl Tween 20 in 100 ml of PBS

**TBST**

Reagents	Concentration
Tris base (1M), pH 8	50ml
Sodium chloride (NaCl) (3M)	100ml
Tween-20	2ml
Distilled water	

**Procedure**

Twelve equal-sized filter papers and nitrocellulose membrane (NC) were taken and properly soaked in transfer buffer. Nitrocellulose membrane was sandwiched between filters papers and gel was placed above the nitrocellulose membrane on the transfer apparatus. Electric current was applied at 10V for 30 minutes. Ponceau staining was done for confirming protein transfer. Afterward, the membrane was then washed with TBST.

### 2.8.6. Blocking

#### Blocking Solution

Blocking solution constituted of the 5% solution of non-fat dry milk prepared in phosphate buffer saline (PBS).

#### Procedure

The membrane was soaked in blocking solution for 45 minutes in order to inhibit nonspecific binding, and then membrane washing was done three times by TBST.

### 2.8.7. Antibody Treatment

#### Primary Antibodies

Proteins	Primary Antibodies
$\alpha$ -tubulin	Mouse monoclonal; Solis BIO
NFATc3	Mouse monoclonal; Santa Cruz
Drp-1	Mouse monoclonal; Santa Cruz
BAX	Mouse monoclonal; Santa Cruz
ET-1	Mouse monoclonal; Santa Cruz

#### Secondary antibodies

Target Proteins	Secondary antibodies
$\alpha$ -tubulin	Goat Antimouse (IGg) Abcam
NFATc3	Goat Antimouse (IGg) Abcam
Drp-1	Goat Antimouse (IGg) Abcam
BAX	Goat Antimouse (IGg) Abcam

#### Dilution of Antibody Solution

0.01% Bovine serum albumin in TBST
------------------------------------

The dilutions of primary and secondary antibodies were made at ratio of 1:5000 and 1:2000 respectively.

### Final Washing Buffer

Reagents	Concentration (mM)
Tris HCl	50
NaCl	150
Distilled water	

### Procedure

Primary antibody treatment was given to nitrocellulose membrane and overnight incubated on the shaker at -4 °C. This is followed by washing three times with TBST. Secondary antibody treatment was given to membrane and incubated on shaker at room temperature for 2 hours. The secondary antibody was discarded afterwards. Finally, NC was washed two times for 5 minutes using final washing buffer.

### 2.8.8. Chromogenic Detection

BCIP (5-bromo 4-chloro 3'-indoly]phosphate)/ NBT (Nitroblue Tetrazolium)
--

### Procedure

1000µl of substrate solution was applied on NC and left it for 30 minutes. Bands were observed after incubation and image is taken. For densitometric analysis, Fiji/imagej software was used.

### 2.9. Quantitative Real Time PCR Analysis

qRT-PCR analysis was done to identify the expression of target genes in the human blood samples and in the rat samples. Following are the steps for PCR analysis:

- RNA extraction from human blood samples and rat's blood and tissue samples

- cDNA synthesis
- qRT-PCR

### 2.9.1. RNA extraction

The extraction of total RNA from the blood and tissues was performed by the protocol mentioned in (Jan et al., 2017).

#### Reagents

Reagents	Volume ( $\mu\text{L}$ )
Trizol	500
Chloroform	50
Isopropanol	150
Glycogen	1
70% Ethanol	500
Diethylpyrocarbonate (DEPC)- treated water	10/25

The samples including both heart and tissue samples were taken from  $-80^{\circ}\text{C}$  and thawed. The samples were centrifuged at 13500rpm at  $4^{\circ}\text{C}$  for 15 minutes and supernatant was removed. In the pellet, 500  $\mu\text{L}$  Trizol was added, and mincing was done with 3 ml syringe. Afterwards, 50  $\mu\text{L}$  of chloroform was added and inversion followed by vortexing was done. The samples were then incubated for 3 minutes at room temperature. Then, the samples were centrifuged at 13500 rpm for 15 minutes at  $4^{\circ}\text{C}$ . After centrifugation, the aqueous layer was separated into the new Eppendorf tube. 150  $\mu\text{L}$  of Isopropanol and 1  $\mu\text{L}$  Glycogen were added to this layer. The samples were then incubated at room temperature for 5 minutes followed by 5 minutes incubation on ice and centrifugation was done afterwards at 13500 rpm at  $4^{\circ}\text{C}$  for 15 minutes. After centrifugation, supernatant was discarded. The pellet collected was washed with 500  $\mu\text{L}$  ethanol and vortexed for 5-10 seconds. Centrifugation was

repeated at 13500 rpm at 4°C for 15 minutes. At the end, Ethanol will be discarded, and the cuvettes are air dried. After proper drying, 10 µL DEPC treated water will be added to dissolve the pellet in case of blood sample and 25 µL DEPC treated water in case of tissue samples.

### 2.9.2. RNA Quantification

After the extraction of RNA, RNA was quantified using Nano V3.7, Thermo fisher Scientific (Nanodrop-1000™). Diethylpyrocarbonate (DEPC)-treated water was used as blank and then the samples were quantified. The A260/A280 value was considered for purification assessment of the RNA sample.

### 2.9.3. cDNA Synthesis

For the synthesis of cDNA from the RNA extracted, “Revert Aid First cDNA Synthesis Kit (Thermo Fisher Scientific, USA)” was used. This synthesis kit had following reagents:

Reagents	Volume
Template RNA	1 µg
Random Hexamer Primer	1 µL
Nuclease Free Water	
10mM dNTP mix	2 µL
Revert Aid M-MuLV RT	1 µL
5X Reaction Buffer (RB)	4.5 µL
Ribolock RNase Inhibitor (RI)	0.5 µL

The kit components were first thawed properly and 12 µL reaction mixture was formed by mixing RNA template, Random Hexamer Primer and Nuclease Free Water in the PCR tube. After this, the PCR tubes was incubated at 65°C for 5 minutes. After incubation, RB, RI, dNTPs and RT was added to make total volume of 20 µL. PCR tubes were then tapped to remove air bubbles followed by incubation in the



thermocycler. PCR cycle involved incubation at 42°C for 60 minutes and then reaction termination phase at 70°C for 5 minutes. After completion of reaction the synthesized cDNA was stored at -20°C until next step.

#### 2.9.4. cDNA dilution

Prior to qRT-PCR, cDNA dilutions (1:4) were prepared. The dilutions were prepared by taking 5  $\mu$ L of cDNA stock in 20  $\mu$ L of Nuclease Free water.

#### 2.9.5. Real Time Polymerase Chain Reaction (qRT-PCR/RT-qPCR)

For qRT-PCR of each individual gene and mi-RNAs, 2  $\mu$ L cDNA dilution was taken for 8  $\mu$ L reaction mixture cocktail making up to the volume of 10  $\mu$ L. For making the reaction mixture following reagents were used:

Reagents	Volume
Nuclease Free Water	2 $\mu$ L
Forward Primer (gene/miRNA specific) (FP)	1 $\mu$ L
Reverse Primer (gene/miRNA specific) (RP)	1 $\mu$ L
Eva Green dye	2 $\mu$ L
cDNA dilution	4 $\mu$ L

At first, the reaction mixture was prepared by adding Nuclease Free Water, FP, RP, and Eva Green dye in the PCR tube. 8  $\mu$ L of reaction mixture and 2  $\mu$ L of cDNA dilution were added in the PCR vials. The PCR vials were then placed in the RT-PCR machine for expression analysis of the selected genes/ miRNA. The program was run and saved on PC. After the reaction completion, Ct values were recorded for each gene or miRNA, and fold activity was calculated.

## 2.10. Fluorescence-based miRNA quantification

For the quantification of miRNA in the blood of normal and CAD patients, the fluorometric method was employed. The qRT-PCR products of miRNA-1a-3p were saved at  $-20^{\circ}\text{C}$  for this experiment. Four samples having mixed Ct values were pooled. 2, 4, 6, 8, and 10% dilutions of pooled samples were made by adding nuclease-free water to make a total  $50\mu\text{l}$  volume. 5% dilutions of control and patients qRT-PCR products were made. In  $50\mu\text{l}$  of each sample,  $50\mu\text{l}$  of  $\text{H}_2\text{O}_2$  was added. Afterward, the fluorescence intensity was measured by using BioTek Synergy HTX microplate reader at 485nm and 520 nm excitation and emission wavelengths respectively. miR-1-3p was quantified in the qRT-PCR products by using the straight-line equation of the standard curve shown in Figure 2.4.

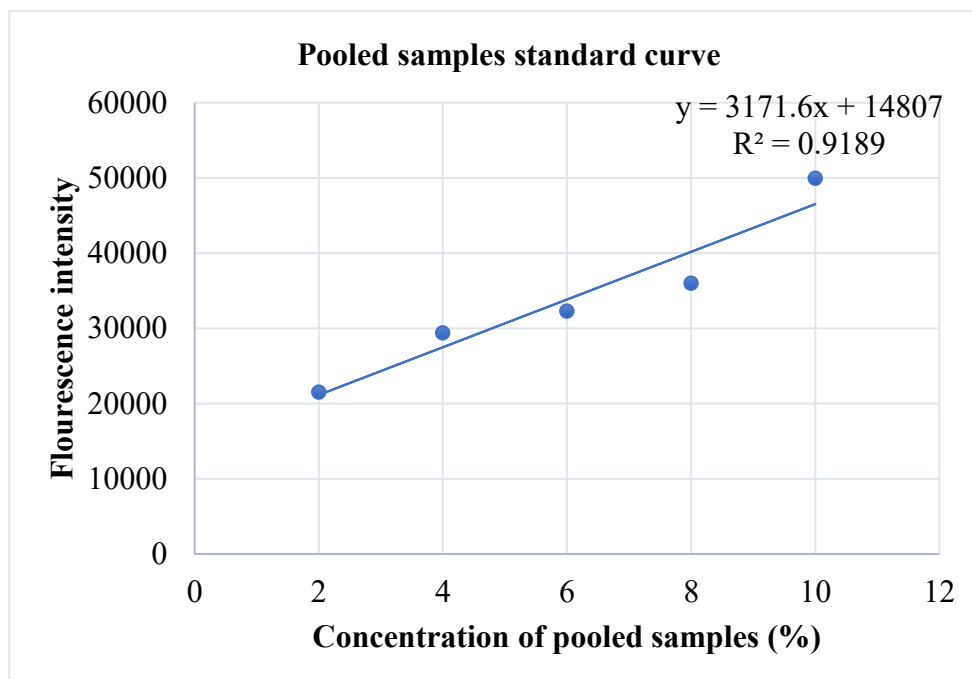


Figure 2.4 Standard Curve for Fluorescence Intensity based Quantification of miRNAs

## 2.11. Oxidative Profiling

For analyzing oxidative profile, Reactive Oxygen Species (ROS) and Thio-barbituric Acid Reactive substances (TBARs) level were investigated.

### 2.11.1. Reactive Oxygen Species (ROS) Assay

Protocol provided by (Hayashi et al., 2007) was followed for detecting ROS level in tissue homogenates and serum samples.

Reagents	Concentration / Volume
Reagent 1: N, N-Diethyl para-phenyl diamine (DEPPD)	1 mg/ ml
Reagent 2: Ferrous sulfate (FeSO <sub>4</sub> )	0.5%
Sodium Acetate Buffer at pH 4.8	0.1 M
Sample	6.6 µl

### Procedure

Reagent mixture was prepared by adding reagent R1 in R2 in 1: 24 ratio and placed in dark for 2 minutes. In each well of microtiter plate, 186 µl reagent mix, 6.6 µl sample and 133.3 µl reaction buffer were loaded. Then, absorbance was recorded at 505 nm using multiskan GO (Thermo-Fischer scientific, USA) spectrophotometer. At the interval of 15 seconds, 3 readings were taken. A standard curve of H<sub>2</sub>O<sub>2</sub> was then generated.

#### 2.11.2. Thio-barbituric acid Reactive substances (TBARs) level

The protocol given by (Tsai et al., 2014) was used to estimate TBARs activity in homogenates and serum samples.

Reagents	Concentration / volume
Tris -HCL	150 mM
Ferrous sulphate	1 mM
Ascorbic acid	1.5 mM
Trichloroacetic acid	10%
Thio-barbituric acid	0.375%
Sample	20 µl

20 µl of each sample, Tris HCL, FeSO<sub>4</sub>, and ascorbic acid along with 120 µl distilled water was taken and incubated for 15 min at 37 °C in an Eppendorf. 200 µl TCA and TBA were then added into it followed by incubation at 100°C for 15 min. This is followed by 10 minutes centrifugation at 3000 rpm. 200 µl supernatant was then picked and added to each well of microtiter plate. Three consecutive absorbances were recorded at 532 nm using multiskan GO. Using the following formula, lipid per oxidation level was calculated:

$$TBARS \left( \frac{nM}{mg} \text{ of protein} \right) = O.D \times total\ volume \times 1.56 \times 105 \times mg\ of\ protein/ml$$

## 2.12. Estimation of Antioxidative Profile

### 2.12.1. Super Oxide Dismutase (SOD) Assay

Using the protocol of (Ali, Waheed, et al., 2015) SOD activity was measured using serum and tissue homogenates samples.

Reagents	Concentration
Phosphate buffer saline (PBS)	50 mM at pH 7.8
L-Methionine	9.9 mM
NBT	57 µM
Triton	0.025 %
Riboflavin	0.9 µM
Sample	5 µl

### Procedure

1.5 ml of L-methionine, 1 ml of NBT.2HCL and 750 µl Triton x-100 was taken and the volume was raised up to 30 ml by adding PBS to make reaction mixture. In each well of micro titer plate, 250µl reaction mixture was added along with 5 µl serum sample.

The microtiter plate was illuminated under fluorescent lamp for 7 minutes at 37 °C. Finally, 2 µl of Riboflavin (chilled) was added into the wells. For initiating the reaction plate was incubated at 40 °C for 8 minutes. Three readings of absorbance were recorded for each sample by using multiskan GO (Thermo-Fischer scientific, USA) spectrophotometer at 560 nm with the time interval of 1 minute.

Percentage inhibition of NBT was calculated by formula mentioned below.

***%age inhibition of NBT***

$$= \left[ \frac{\text{Abs Blank} - \text{Abs Sample}}{\text{Abs. (blank)}} \right] \times 100$$

**2.12.2. Catalase Activity (CAT) Assay**

Protocol described by (Ali, Shaheen, et al., 2015) was used to estimate the activity of CAT enzyme using following reagents:

Reagents	Concentration / Volume
Distilled hydrogen per oxide	5.9 mM
Potassium phosphate buffer	50 mM at pH 7
Samples	11.1 µl

**Procedure**

222 µl of buffer, 111 µl of H<sub>2</sub>O<sub>2</sub> and 11.1 µl of serum sample were poured in each well of microtiter plate. For blank, all the reagents except sample were added. Three absorbance readings were recorded at 240 nm by multiskan GO spectrophotometer.

**2.12.3. Peroxidase (POD) Assay**

POD assay was performed according to the protocol mentioned by (Ishtiaq et al., 2020).

**Reagents**

Reagents	Concentration / Volume

Phosphate buffer	50 mM, pH 5.0
H <sub>2</sub> O <sub>2</sub>	40 mM
Guaiacol	20 mM
Samples	6.7 $\mu$ l

### Procedure

In each well of microtiter plate, 166.6  $\mu$ l phosphate buffer, 6.7  $\mu$ l (50 mM) Guaiacol and 6.7  $\mu$ l sample were added respectively followed by vigorous shaking. Finally, H<sub>2</sub>O<sub>2</sub> was added. Three readings of absorbance were recorded at 420 nm with the interval of 1 minute using multiskan GO (Thermo-Fischer scientific, USA) spectrophotometer.

#### 2.12.4. Ascorbate Peroxidase (APX) Assay

This assay was performed according to the protocol mentioned by (Nakano & Asada, 1981).

Reagents	Concentration / Volume
Potassium phosphate buffer	50 mM, pH 7
EDTA	5 mM
Ascorbate	1 mM
H <sub>2</sub> O <sub>2</sub>	1 mM
Sample	10 $\mu$ l

### Procedure

60  $\mu$ l potassium phosphate buffer, 10  $\mu$ l of EDTA, 10  $\mu$ l Ascorbate, 10  $\mu$ l H<sub>2</sub>O<sub>2</sub> alongwith 10  $\mu$ l of sample were taken in wells of microtiter plate. Three absorbance readings were recorded at 290 nm by multiskan GO spectrophotometer. Level of ascorbate peroxidase was estimated using following formula:

**Ascorbate activity**

$$= \text{Absorbance} \times \text{Extinction coefficient of Ascorbate}$$

**2.12.5. Reduced Glutathione Assay**

The measurement of GSH was done according to the protocol of (Jollow, Mitchell, Zampaglione, & Gillette, 1974).

**Reagents**

Reagents	Concentration
3,3-dithi-bis (6-nitrobenzoic acid) DTNB	0.4%
Sodium Phosphate buffer	11.356 g, 0.4 M
Serum sample	5 $\mu$ l

**Procedure**

In each well of microtiter plate 5  $\mu$ l sample, 50  $\mu$ l sodium phosphate and 25  $\mu$ l DTNB were added this resulted in yellow colour. Absorbance was measured at 412 nm by multiskan GO spectrophotometer.

**2.13. Lipid profile**

For assessing the lipid profile triglyceride and cholesterol assays were performed.

**2.13.1. Cholesterol assay**

According to the protocol given in AMP (AMEDA Labordiagnostik GmbH; Austria) diagnostic kit, cholesterol assay was performed.

**Principle**

The reaction mixture containing 4-aminoantipyrine and phenol can get condensed by enzymes having hydrogen peroxides including peroxidase, cholesterol oxidase and cholesterol esterase. This results in the formation of quinonimine dye. The amount of cholesterol in sample is directly proportional to concentration of quinonimine dye.

Reagents	Volume
Cholesterol reagent	200 $\mu$ l
Sample	2 $\mu$ l
Standard	2 $\mu$ l

### Procedure

In each well of the microtiter plate, 200  $\mu$ l of reagent along with 2  $\mu$ l sample was added. In a separate well, 2  $\mu$ l of standard in 200  $\mu$ l of reagent was also added. Absorbance of sample and standard was taken at 500 nm using from multiskan GO spectrophotometer three times after incubating at 37 °C for 5 minutes. Total cholesterol levels were estimated using the kit formula.

$$\text{total cholesterol } \left( \frac{\text{mg}}{\text{dL}} \right) = \frac{\text{sample absorption}}{\text{standard absorption}} \times \text{concentration of standard}$$

### 2.13.2. Triglycerides

According to the protocol given in AMP (AMEDA Labordiagnostik GmbH; Austria) kit, triglycerides assay was performed using the following reagents:

Reagents	Volume
Triglyceride reagent	200 $\mu$ l
Sample	2 $\mu$ l
Standard	2 $\mu$ l

### Principle

Triglycerides are broken down into fatty acid and glycerol. This glycerol is phosphorylated in the presence of ATP into glycerol-3-phosphate (G-3-P) by glycerol kinase (GK). This G-3-P is oxidized by glycerol phosphate oxidase enzyme in to dihydroxy acetone phosphate (DHAP) and H<sub>2</sub>O<sub>2</sub>. H<sub>2</sub>O<sub>2</sub> reacts with 4-amino-antipyrine,



and phenol and this reaction is catalyzed by POD that eventually produces red color. The color intensity is directly proportional to the concentration of triglycerides in the sample.

### Procedure

In each well of the microtiter plate, 200  $\mu$ l of reagent along-with 2  $\mu$ l sample was added. In a separate well, 2  $\mu$ l of standard in 200  $\mu$ l of reagent was also added. Absorbance of sample and standard was taken at 500 nm using from multiskan GO spectrophotometer three times after incubating at 37 °C for 5 minutes. Total triglycerides levels were estimated using the kit formula.

$$\text{Total triglycerides } \left( \frac{\text{mg}}{\text{dL}} \right) = \frac{\text{sample absorption}}{\text{standard absorption}} \times \text{concentration of standard}$$

### 2.14. Liver function tests

To analyze liver functions, ALT and AST assays were performed.

#### 2.14.1. Alanine Aminotransferase (ALT) Assay

The protocol given by AMP (AMEDA Labordiagnostik GmbH; Austria) diagnostic kit was used to estimate ALT enzymes levels in serum.

Reagents	Concentrations / Volume
Reagent 1 (Tris-buffer, L-Alanine, Lactate dehydrogenase)	150 mM PH 7.3, 750 mM > 1.350 U/L
Reagent 2 (NADH, 2-Oxoglutarate, Biocides)	1.3 mM, 75 mM
Serum sample	10 $\mu$ l

### Procedure

To prepare reaction mixture, R1 and R2 were mixed in 4:1. 200  $\mu$ l of reaction mixture was added in each well, 10  $\mu$ l sample was poured and incubated for 1 min at room

temperature. Afterwards, absorbance was recorded at 340 nm wavelength by multiskan GO spectrophotometer. To calculate 3 readings, the same steps of incubation were repeated. Using the formula given in the kit, level of ALT in serum was calculated.

$$\frac{\Delta A}{\text{min}} \times 3333 = \text{ALT activity} \left( \frac{\text{unit}}{\text{liter}} \right)$$

### 2.14.2. Aspartate Aminotransferase (AST) assay

The protocol given by AMP (AMEDA Labordiagnostik GmbH; Austria) diagnostic kit was used to estimate AST enzymes levels in serum.

#### Principle

Aspartate amino transferase catalyzes the (amino) NH<sub>3</sub> group transfer from L-aspartate to alpha-ketoglutarate and forms oxaloacetate and L-glutamate. Malate dehydrogenase (MDH) reduces oxaloacetate and results in oxidation of NADH to NAD<sup>+</sup> hence decreasing the absorption. The activity of AST is proportional to absorption.

#### Reagents

Reagents	Concentrations / Volume
Reagent 1 (Tris-buffer, L-aspartate, NADPH, MDH, LDH)	121 mM PH 7.8, 362 mM > 460 U/L, >600 U/L
Reagent 2 (NADH, 2-Oxoglutarate, Biocides)	1.3 mM, 75 mM
Sample	10 µl

#### Procedure

To prepare reaction mixture, R1 and R2 were mixed in 4:1. 200 µl of reaction mixture was added in each well, 10 µl sample was poured and incubated for 1 min at room temperature. Afterwards, absorbance was recorded at 340 nm by multiskan GO (Thermo Fischer scientific, USA) spectrophotometer. To calculate 3 readings, the same

steps of incubation were repeated. Using the formula given in the kit, the activity of ALT in serum was calculated.

$$\frac{\Delta A}{\text{min}} \times 3333 = \text{ALT activity} \left( \frac{\text{unit}}{\text{liter}} \right)$$

### **2.15. Statistical Analysis**

For statistical analysis, one way ANOVA (Analysis of Variance) proceeded by Tukey's Test (t-test) was employed. p-value of  $\leq 0.01$  or  $\leq 0.05$  were considered significant, that were calculated by using GraphPad Prism version 10.0.0. The graphs were made using the Graphpad Prism software.

### **2.16. Histopathology**

For microscopic analysis, tissues were fixed in fixative-form of formaldehyde 30 %, absolute alcohol 60 % and acetic acid 10 %-which was proceeded by dissection. At normal room temperature, the fixed tissues were shifted into cedar wood oil until it turned crystal clear. These tissue implants were then shifted into liquid wax. Bubbles were removed and wax was allowed to harden. A chunk of wax imbedded tissues was made. Using disinfected blade, the piece of paraffin wax was cut and for segmenting tissue is placed on wooden slab.

#### **2.16.1. Microtomy**

A tissue placed on wooden slab was cut off into 5 $\mu$ m thin slices by using microtome and were extended and fixed. These slices along with wax strips were transferred in water bath at 60°C. This results in smooth transferred on to glass slide. Fixation of tissues on slide was done by liquefying the wax at 65°C which were followed by incubation for 24 hours then tainted with hematoxylin.

#### **2.16.2. Microscopic Analysis**

At 40 X magnification, glass slides were observed using a light microscope (DIALUX 20 EB). All the slides were observed and photographed

### 3. RESULTS

#### 3.1. Research Summary

In our study, the expression of several miRNAs and genes involved in apoptotic signaling pathways was assessed and miRNA mimics were used for target gene confirmation. Biochemical assays were performed to analyze oxidative stress, lipid status and liver function profile in rats. qRT-PCR was conducted to validate the mRNA expression levels. Western blotting was conducted to validate protein level expression of apoptotic signaling modulators and confirm miRNA target genes in diseased model. Histological analysis was also performed to analyze the cellular architecture.

#### 3.2. Demographic Data of Patients

##### 3.2.1. Gender-wise Distribution

The CAD patients were divided in two groups based on gender as shown in Figure 3.1. The first group comprised male patients making 72.72%. The second group comprised of female CAD patients making 27.27% as shown in Table 3.1.

Table 3.1 Gender-wise distribution of CAD Patients

Gender	Percentage
Male	72.72%
Female	27.27%

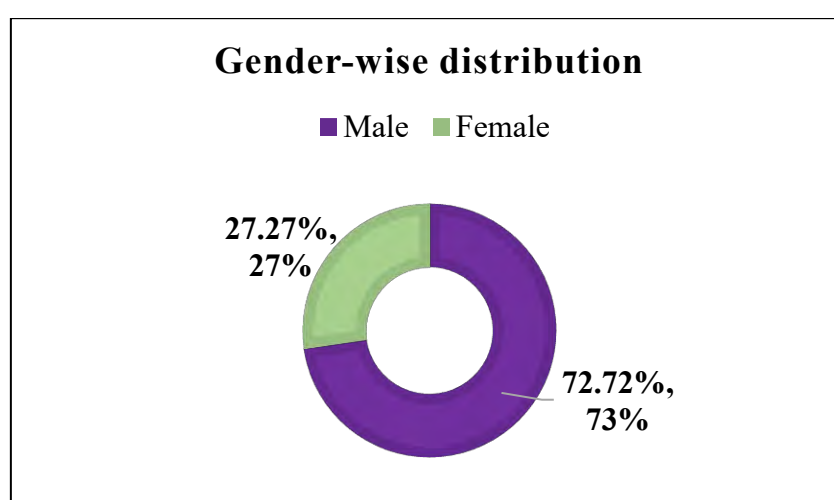


Figure 3.1 Graphical Representation of Gender-wise Distribution of CAD Patients

### 3.2.2. Age-wise Distribution

The CAD patients were distributed into four groups based on age as shown in Figure 3.2. The first group was comprised of CAD patients with age < 20. Second group was consisted of CAD patients between ages 21-40. Third group was consisted of CAD patients between the ages of 41-60. The fourth group was comprised of CAD patients above age 60 as shown in Table 3.2.

Table 3.2 Graphical Representation of Age-wise Distribution of CAD Patients

Age Group	Percentage
< 20	9.09%
21-40	18.18%
41-60	27.27%
> 60	45.45%
<b>Grand Total</b>	<b>100%</b>

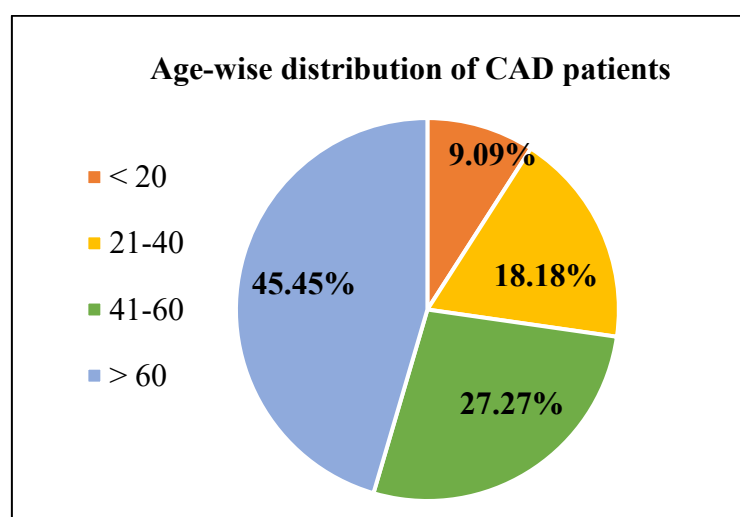


Figure 3.2 Graphical Representation of Age-wise Distribution of CAD Patients

### 3.2.3. Other Diseases in CAD Patients

27.27% of CAD patients were suffering from diabetes and 45.45% of CAD patients were suffering from hypertension.

Table 3.3 Other Diseases in CAD Patients

	Percentage
<b>Diabetes</b>	27.27%
<b>Hypertension</b>	45.45%

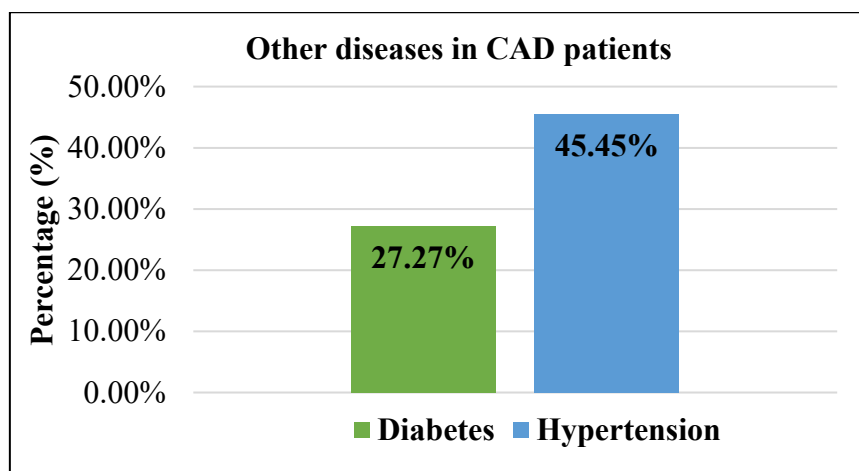


Figure 3.3 Graphical Representation of other diseases in CAD Patients

### 3.2.4. Smoking Status in CAD Patients

27.27% CAD patients were smokers while others were non-smokers as shown in Table 3.4.

Table 3.4 Smoking Status in CAD Patients

	Percentage
<b>Smokers</b>	27.27%
<b>Non-Smokers</b>	72.72%

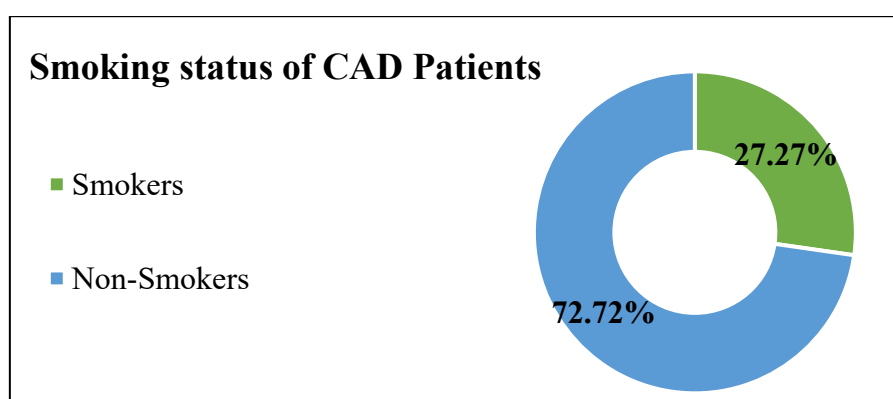


Figure 3.4 Graphical Representation of Smoking Status in CAD Patients

### 3.3. Relative expression analysis of miRNAs and target genes in CAD Patients

miRNAs are used as the diagnostic biomarker for various pathologies including CVDs, and cancers. In this study, relative expression analysis of miR-1-3p, and miR-98-5p was done using RT-qPCR in control and CAD patient groups.

#### 3.3.1. Increased expression of miR-1-3p in CAD Patients

miR-1-3p is reported to be elevated in CVDs including MI and cardiac ischemia. To validate the expression of miR-1-3p in CAD patients, qRT-PCR was used. The expression of miR-1-3p was analyzed using U6 as an internal control. miR-1-3p expression level was considerably increased in the CAD patients' group in contrast to the Control group. T-test was performed to analyze the data statistically using GraphPad Prism 10.0.0 software. Results are depicted in Figure 3.5 as Mean  $\pm$  Standard Error Mean (SEM), (\*\*\*) at  $p$ -value  $<0.001$ .

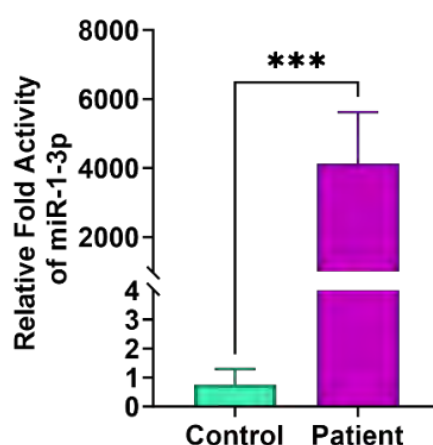


Figure 3.5 Graphical showing the Fold activity of miR-1-3p in Human Blood sample

#### 3.3.2. Decreased expression of miR-98-5p in CAD Patients

miR-98-5p is reported as an important transcriptional regulator of various important genes involved in psychological and pathological conditions. The validation of miR-98-5p in CAD was done using U6 as an internal normalization control, the relative fold activity of miR-98-5p was found to be considerably downregulated in CAD patients. The results with (\*\*) at  $p$ -value  $<0.01$  are plotted with Mean  $\pm$  SEM in Figure 3.6.

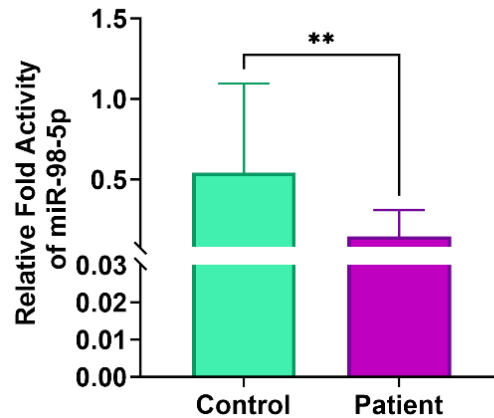


Figure 3.6 Graphical showing the Relative fold activity of miR-98-5p in Human Blood sample

### 3.3.3. mRNA expression analysis of genes as putative miRNA targets

For evaluating the effects of miRNA expression dysregulation in CAD patients, the expression of their target genes by qRT-PCR was done. The results showed the role of miRNAs in dysregulating the physiological pathways modulators, leading to CAD development.

### 3.3.4. Reduced expression of NFATc3 in CAD Patients

According to the TargetScan Human database, NFATc3 was found to be the putative target for miR-1-3p (Figure 3.9). GAPDH was used as an endogenous control. The results confirmed that the relative expression of NFATc3 was significantly downregulated in patients with CAD. Increased expression of miR-1-3p and downregulation of NFATc3 expression suggests NFATc3 as a putative target gene of miRNA-1-3p. T-test was performed, and the results are plotted as Mean±SEM with (\*\*\*\*) at  $p$ -value<0.0001.

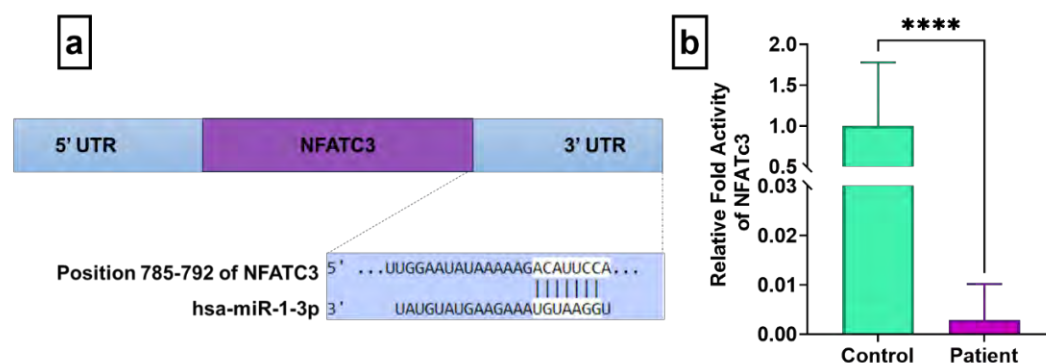


Figure 3.7 a) Target site Prediction by Bioinformatics Database b) Relative Fold Activity of NFATc3



### 3.3.5. Decreased expression of Bcl-2 in CAD Patients

Bcl-2 is an anti-apoptotic protein involved in regulating cellular apoptosis in cardiac ischemia (Korshunova et al., 2021). Results showed that mRNA expression level of Bcl-2 was significantly downregulated in CAD patients. GAPDH was used as an endogenous control. The statistical analysis was performed on GraphPad Prism 10.0.0 Software by t-test. A graph was plotted based on Mean $\pm$ SEM with \*\*\*\* at *p*-value <0.0001 shown in Figure 3.8.

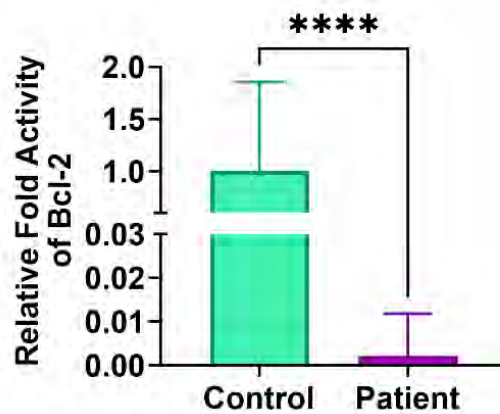


Figure 3.8 Relative Fold Activity of Bcl-2

### 3.3.6. Upregulated expression of BAX in CAD Patients

BAX is an apoptotic protein and a key player in apoptotic signaling pathways involved in CAD development and progression. The mRNA expression level of BAX was assessed using GAPDH as an internal control. A remarkable increase in relative the fold activity of BAX was observed in CAD patient's group suggesting the apoptosis in CAD patients. T-test was performed and the results are shown in figure 3.9.

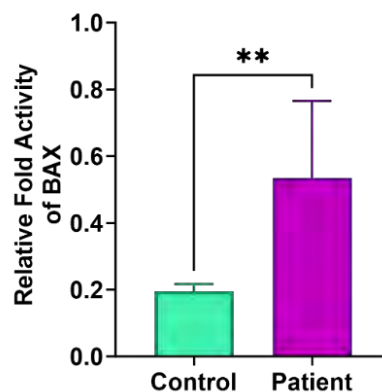


Figure 3.9 Relative Fold Activity of BAX

### 3.3.7. Increased expression of ET-1 in CAD Patients

Bioinformatics analysis by using TargetScanHuman database showed ET-1 as the potential target gene of miR-98-5p and miR-1-3p. qRT-PCR results confirmed that ET-1 was upregulated in CAD patients. GAPDH was used as an internal normalization control. The results showed a marked elevation in the ET-1 mRNA expression level in the CAD patients. The results are depicted graphically as Mean $\pm$ SEM with \*\* at *p*-value <0.01 in Figure 3.10.

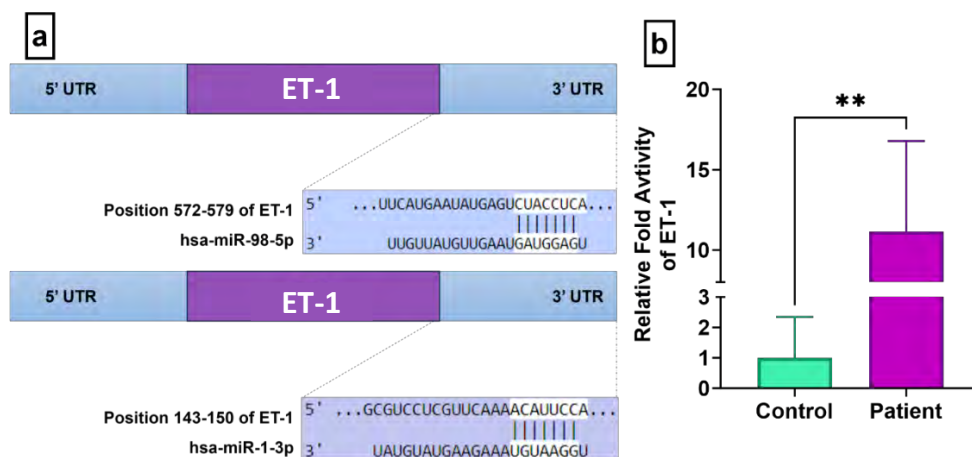


Figure 3.10 a) Target site Prediction by Bioinformatics Database b) Relative Fold Activity of Et-1

### 3.4. Fluorescence-based quantification of miR-1-3p

For the quantification of miRNA in control and patients, the fluorescence detection method was employed. In contrast to the control group, a remarkable increased quantity of miR-1-3p was present in the CAD patients. T-tests were performed and the graphical representation of results is in Figure 3.11.

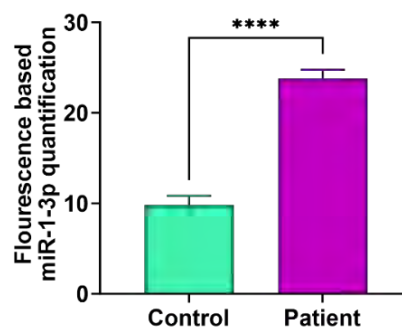


Figure 3.11 Fluorescence Intensity based Quantification of miR-1-3p

### 3.5. Evaluation of ISO induced CAD in animal model

To validate the expression of miRNAs and their putative target genes in diseased conditions, animal model studies were also conducted.

#### 3.5.1. Assessment of Baseline Characteristics in animal model

For the confirmation of the development of the ISO-induced MI model, the weight of heart (HW) to weight of body (BW) ratio and HW to tibia length (TL) ratio was considered. ISO-induced MI rat group showed a marked increase in HW/BW and HW/TL length in contrast to the control rat group. The statistical analysis was performed. Graphs for HW/BW and HW/TL are plotted as Mean $\pm$  SEM with \*\*\* at  $p$ -value < 0.001 and \*\* at  $p$ -value < 0.01 respectively (figure 3.12).

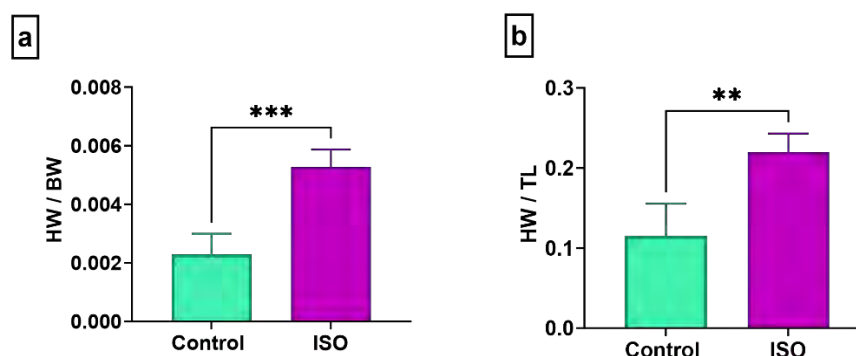


Figure 3.12 a) Heart weight to Body weight ratio of rats b) Heart weight to Tibia length ratio of Rats

#### 3.5.2. Oxidative Stress Profiling for Pathological Confirmation

For confirming the pathological development in the ISO-induced rat group in contrast to the control group, oxidative stress profiling was done by performing various oxidants and antioxidant biochemical assays.

##### 3.5.2.1. Assessment of oxidants level in animal model

For oxidants profiling of rats, ROS and TBARs assays were performed on the serum and homogenates of control and ISO treated rats' heart tissue. The ISO-treated rats showed a notable increase in ROS levels. The ROS levels are plotted as Mean $\pm$ SEM in figure 12. Moreover, lipid peroxidation due to high ROS levels in the ISO group was also confirmed by the TBARs assay. A significant elevation of TBARs level was observed in the ISO group in contrast to the Control group. The results for the TBARs level are depicted in figure 3.13.

### 3.5.2.2. Evaluation of antioxidants enzyme activity in animal model

To confirm the oxidative stress, the antioxidant profiling was done by evaluating the activities of POD, SOD, GSH, CAT and APX antioxidants. These antioxidants have the potential to scavenge potential ROS present within the cell. Under diseased conditions, heart tissue serum as well as homogenates have shown a remarkable decrease in the activities of these antioxidant enzymes thereby increasing oxidative stress. In our study, ISO-induced group showed a significant decrease in the activities of antioxidant enzymes. The results are indicated in figure 3.14 as Mean $\pm$ SEM.

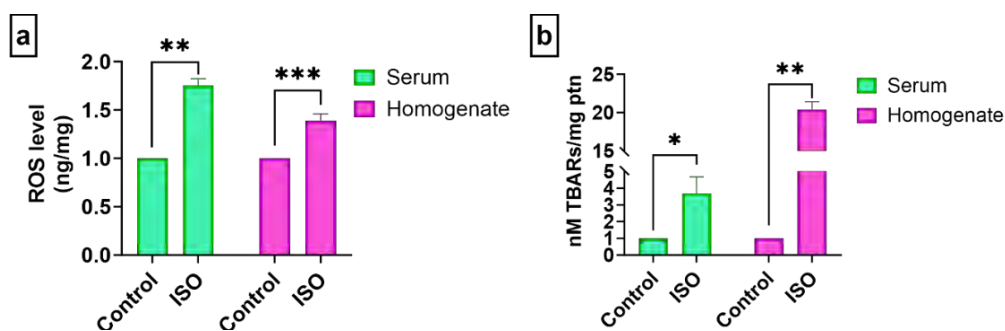


Figure 3.13 a) ROS levels in Rat Serum and Tissue Homogenates b) TBARS level in Rat's Tissues

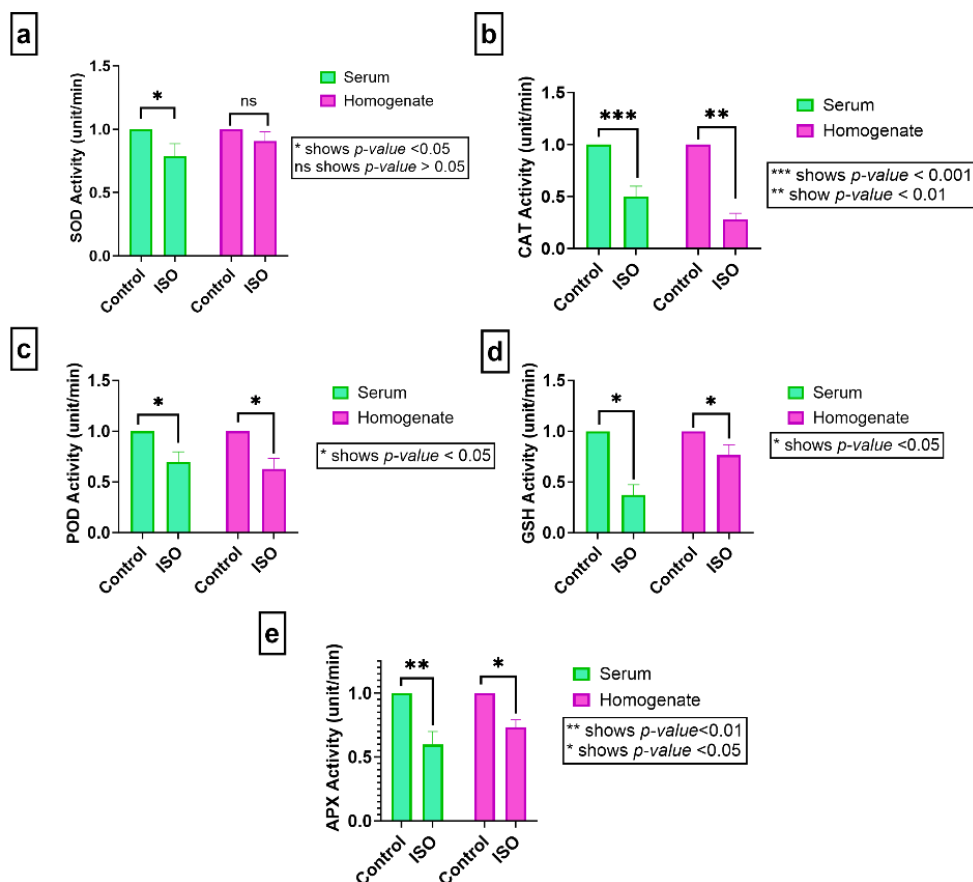


Figure 3.14 Antioxidants Profile a) SOD activity level, b) CAT activity level, c) POD activity level, d) GSH activity level e) APX activity level

### 3.5.3. Assessment of liver function tests in animal model

To assess liver functioning and liver damage in normal and diseased rats, liver function tests were performed. ALT and AST levels were evaluated in the serum of normal and diseased rats. All the results were statistically analyzed. Both AST and ALT levels were found to be remarkably elevated in the diseased rats. Increased ALT and AST serum levels showed liver damage in ISO-induced rats' groups. The results are depicted graphically in Figure 3.15.

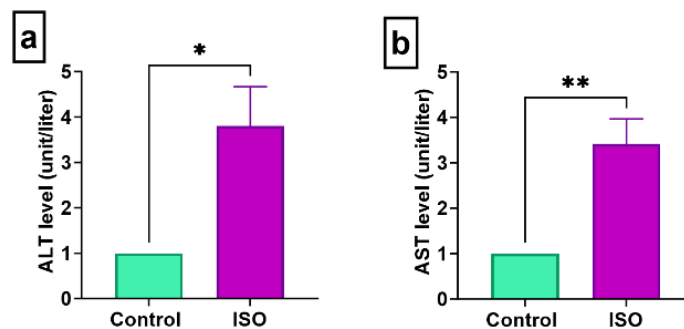


Figure 3.15 Graphical Representation of Liver Function Tests a) ALT level (unit/min) b) AST level (unit/min)

### 3.5.4. Evaluation of lipids level in animal model

In CAD, increased peripheral lipids play a pioneer and important part in the development and progression of the disease. To confirm the correlation of lipids with the disease, and lipid metabolism with CAD, triglycerides and cholesterol levels were assessed using biochemical assays. The results are statistically analyzed by performing t-tests. The results showed a significant increase in the levels of TGs and cholesterol in the serum of ISO rats. Increased levels are indicative of an association between lipid metabolism and cardiotoxicity. The results are shown as Mean $\pm$ SEM in Figure 3.16.

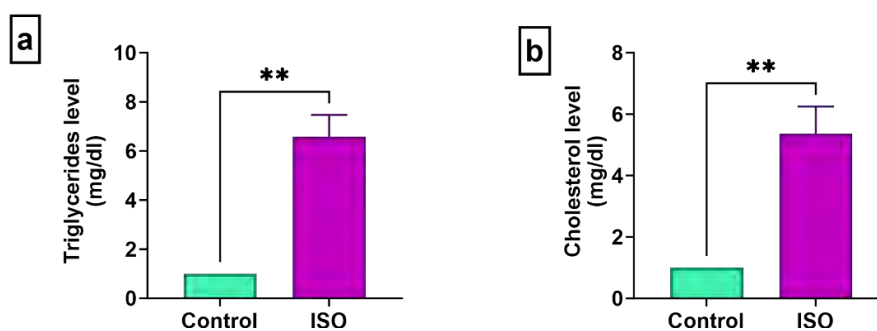


Figure 3.16 Graphical Representation of Lipid Profile a) Triglycerides level (mg/dl) b) Cholesterol level (mg/dl)

### 3.5.5. Analysis of mRNA/miRNA expression in animal model

#### 3.5.5.1. Increased miR-1-3p expression in ISO induced animal model

The level of miR-1-3p expression in heart tissue of rats was assessed. Using U6 as an endogenous control, the results of qRT-PCR were analyzed. Statistical analysis using t-tests showed that the ISO group has a decreased expression level of miR-1-3p in the heart tissue samples. The results are depicted in figure 3.17.

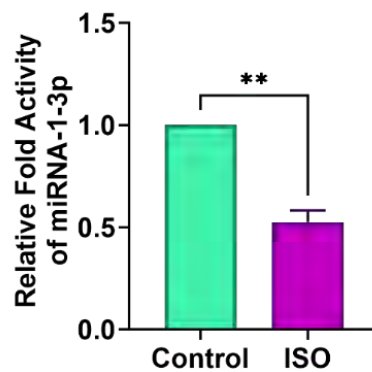


Figure 3.17 Relative fold activity of miR-1-3p in Rat Heart tissue sample

#### 3.5.5.2. Decreased miR-98-5p expression in ISO induced animal model

The expression level of miR-98-5p in Rat's blood and heart tissue were evaluated by qRT-PCR. Using U6 as an endogenous control, the results were evaluated. The T-test was performed using GraphPad Prism. The relative fold activity of miR-98-5p was found to be significantly decreased in blood as well as in the heart tissue of rats. The results are depicted in Figure 3.18 as Mean±SEM.

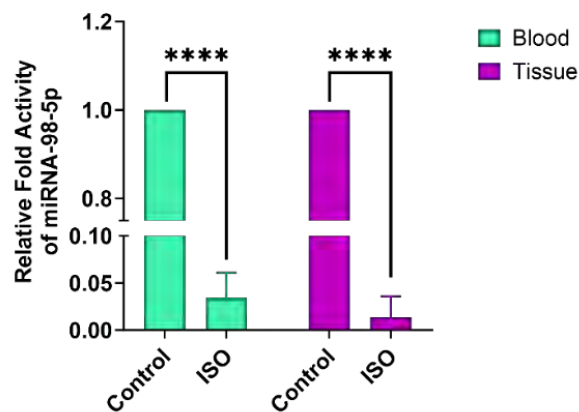


Figure 3.18 Relative fold activity of miR-98-5p in Rats Blood and Heart Tissues

### 3.5.5.3. Dysregulated NFATc3 expression in ISO-induced animal model

As a potential target of miR-1-3p and having a role in pathogenesis, NFATc3 relative fold activity was validated in both blood and heart tissue sample. A remarkable decrease in the relative fold activity of NFATc3 was observed in blood samples while an increased level was observed in heart tissue samples. The t-test was performed and the results are plotted as Mean $\pm$ SEM in Figure 3.19.

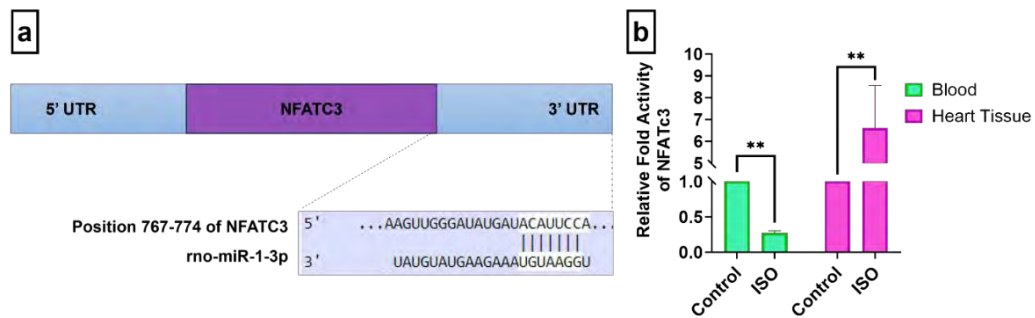


Figure 3.19 a) Target site Prediction by Bioinformatics Database b) Relative Fold Activity of NFAT-c3 in Rat's Tissues

### 3.5.5.4. Upregulated Et-1 expression in ISO-induced Rat's Tissues

Et-1 was predicted as a potential target of miR-98-5p and miR-1-3p by the bioinformatics tool. The mRNA expression levels of Et-1 were assessed in both the blood and heart tissue of rats. The results showed an elevated level of Et-1 in both the blood and heart tissue of the ISO-induced rats. Increased Et-1 showed endothelial dysfunction in the ISO group. The results are depicted in Figure 3.20 as Mean $\pm$ SEM at \* with *p*-value <0.5.

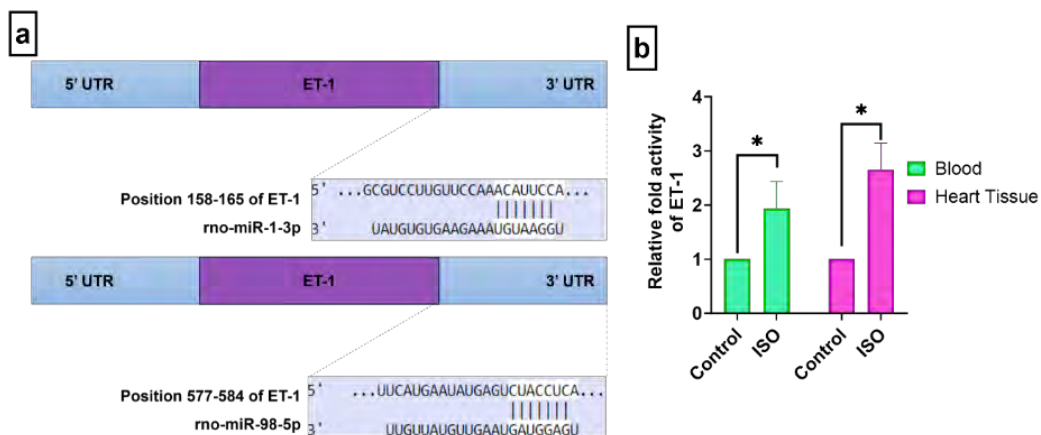


Figure 3.20 a) Target site Prediction by Bioinformatics Database b) Relative Fold Activity of ET-1 in blood and heart tissue of rats

### 3.5.5.5. Downregulated Bcl-2 expression in ISO-induced Rat's Tissues

The relative fold activity of Bcl-2 was assessed as a downstream modulator of NFATc3 and an anti-apoptotic marker. Both the tissues including the blood and heart tissue depicted a remarkable decrease in the relative fold activity of Bcl-2. Graphs are plotted after performing t-test on the data of both groups and are plotted in Figure 3.21.

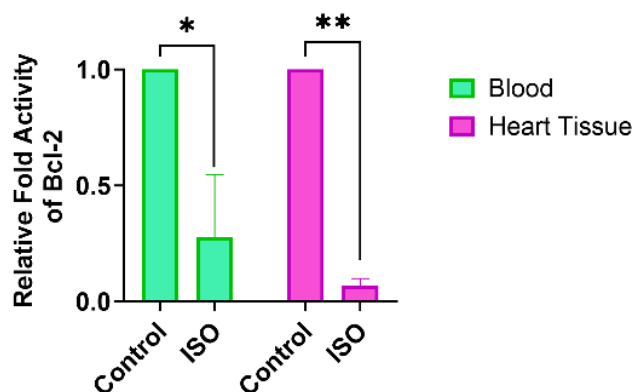


Figure 3.21 Relative Fold Activity of Bcl-2 in Rat's Tissues

### 3.5.5.6. Upregulated Bax expression in ISO-induced Rat's Tissues

The relative fold activity of Bax was assessed as a pro-apoptotic marker. The heart tissue depicted a remarkable increase in the relative fold activity of Bax suggesting apoptosis. Graphs are plotted after performing t-test on the data and are presented in Figure 3.22.

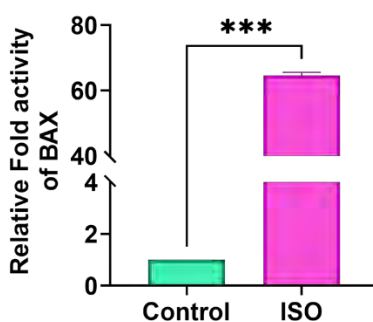


Figure 3.22 Relative Fold Activity of Bax in Rat's heart tissue

### 3.5.6. Evaluation of Protein Expression Analysis in ISO induced rat model

Western Blotting was performed to analyze the level of apoptotic protein expression included in and the validation of protein expression dysregulated by miRNAs.



### 3.5.6.1. Increased NFATc3 protein expression in ISO group

NFATc3 is a major potential target of miR-1-3p. NFATc3 protein level were evaluated by western blotting. Densitometric analysis was done using ImageJ software.  $\alpha$ -tubulin was used as a normalization control. The results showed a remarkably increased relative expression of NFATc3 in the ISO-induced rat model. The groups of ISO+miR-98-5p mimic and miR-98-5p mimic showed a relative decrease in the expression of NFATc3. This showed that a dose of miR-98-5p mimic can also reduce NFATc3 expression. The results are plotted after performing One-way ANOVA and Multiple Comparisons in GraphPad Prism 10.0.0 and are depicted as Mean $\pm$ SEM in Figure 3.23.

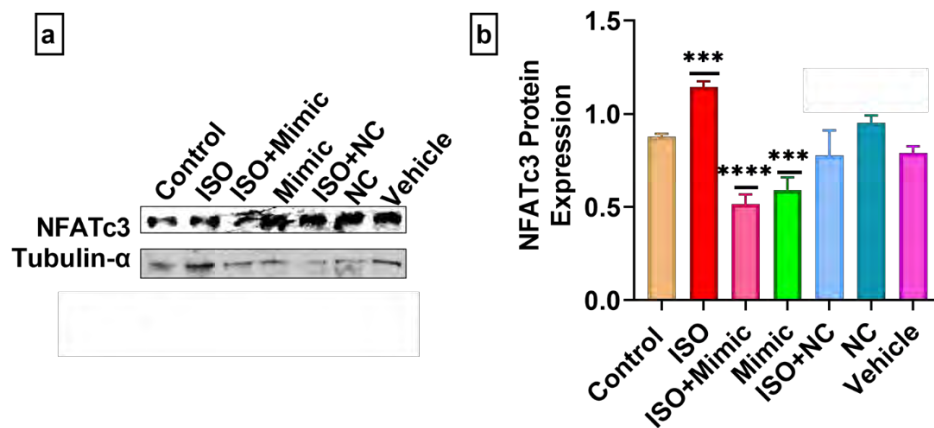


Figure 3.23 a) Western Blot image for NFAT b) Graphical Representation of NFATc3 protein expression

### 3.5.6.2. Upregulated BAX protein expression in ISO group

BAX is an important player in apoptotic pathways. Western Blotting was performed to validate the relative protein level of BAX in control, disease, and miRNA-mimic groups. Densitometric analysis was followed by statistical analysis using t-test. The results depicted a significant elevated in the relative protein expression level of BAX in the ISO group. This suggested increased apoptosis in cardiomyocytes in the case of ISO-induced MI. In contrast to ISO group, the levels of BAX in ISO+miR-98-5p mimic and miR-98-5p mimic groups were found to be significantly downregulated. This showed that miR-98-5p mimic is involved in regulation of the apoptosis signaling in cardiomyocytes. The results are depicted in figure 3.24 as Mean $\pm$ SEM.

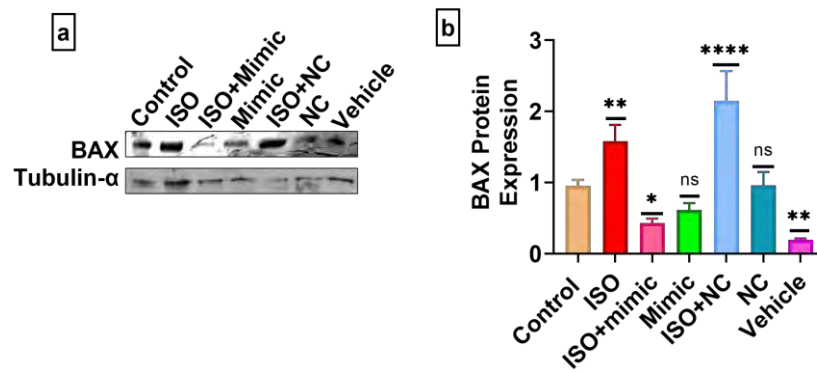


Figure 3.24 a) Western Blot image for BAX b) Graphical Representation of BAX protein expression

### 3.5.6.3. Upregulated Drp-1 protein expression in ISO group

Drp-1 is a marker of mitophagy and mitochondria-associated apoptosis. The expression of Drp-1 was validated by western blotting. A significant increase in protein expression of Drp-1 was observed in the ISO group, indicating mitochondria-associated apoptosis. The expression of Drp-1 in miR-98-5p mimic groups was found to be significantly diminished. The results are shown as Mean±SEM in Figure 3.25.

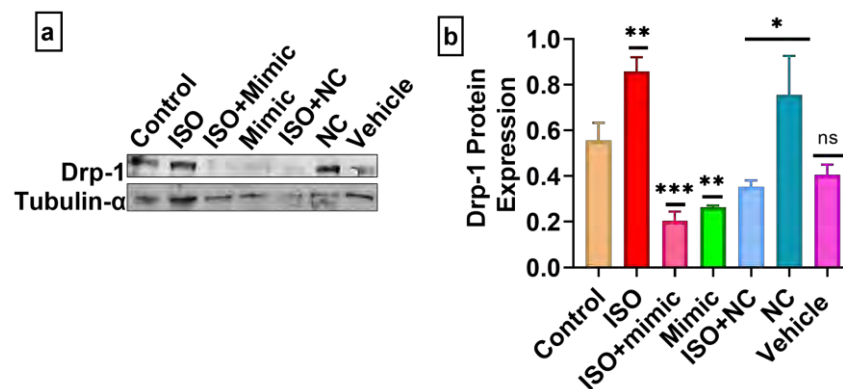


Figure 3.25 Western Blotting for Drp-1 a) Western blot image b) Graphical representation of Drp-1 protein expression level

### 3.5.6.4. Upregulated Et-1 protein expression in ISO group

Et-1 is the direct putative target of miR-98-5p and is reported to be involved in the initial stages of CAD development. The expression of Et-1 was found to be drastically increased in case of ISO group. ISO+mimic and mimic groups have shown a remarkable decrease in Et-1 levels. This showed that miR-98-5p mimics reduced the expression of Et-1. The results are indicated in Figure 3.26 as Mean±SEM.

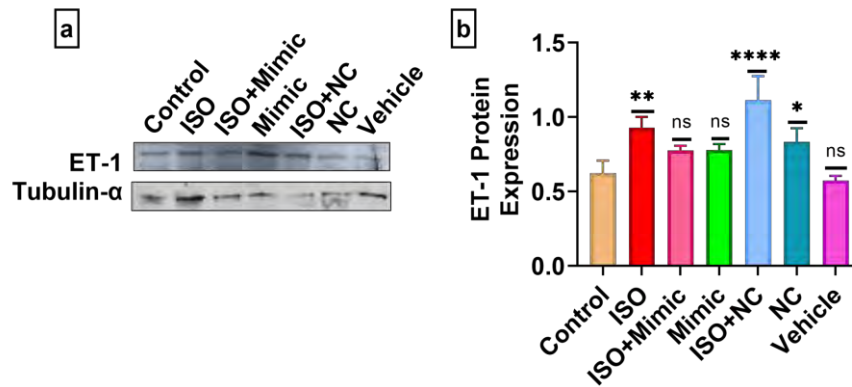


Figure 3.26 a) Image of the Western Blot b) Graph showing ET-1 protein expression.

### 3.5.7. Histological investigation of Rat's Heart tissue

After H&E staining of rat's heart tissue, the microscopic analysis was performed. The cells in ISO group showed altered morphology with an increase in cell size showing hypertrophic cells. The cardiac muscle fibers were found to be distantly spaced in ISO in comparison to the control group. The percentage abnormal cells was observed to be elevated in ISO gro. (Figure 3.27)

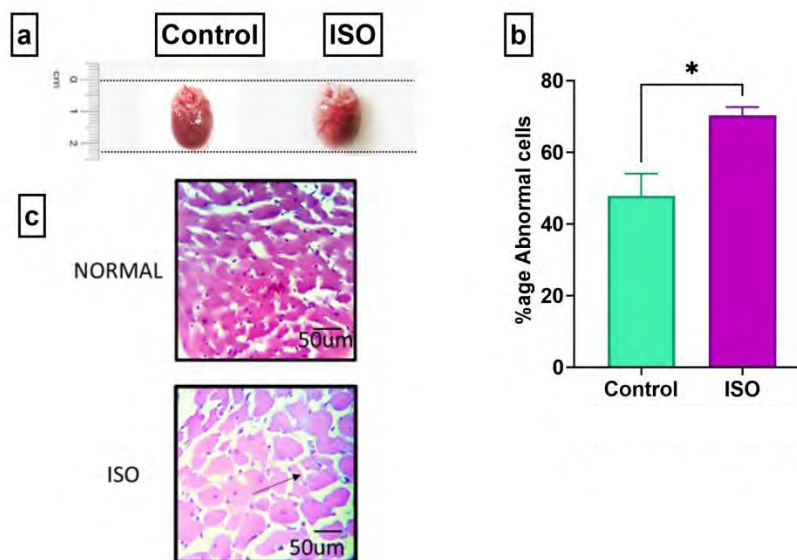


Figure 3.27 a) Images of Control and ISO rats hearts b) H&E staining images of control and ISO rats c) Graphical Representation of Percentage Abnormal cells in Normal control and ISO hearts

## 4. DISCUSSION

According to the World Heart Report 2023, 85% of the total CVDs associated deaths are caused by CAD and stroke. 9.1 million deaths are reported due to ischemic heart disease or CAD by the World Heart Federation (*World Heart Report 2023*). CAD is said to be the primary disease that eventually leads to MI. Early diagnosis of CAD may enable better management of this disease. The diagnostic strategies that are currently being used have various problems associated with them. miRNAs can provide a better diagnostic option and can be used as an earlier biomarker for CAD. We conducted our study on both human and animal models. Our study involves the elucidation of miR-1-3p and miR-98-5p levels in CAD patients. miR-1-3p is previously reported to be involved in atherogenesis and prognosis of CAD (Badacz et al., 2021) while miR-98-5p was not extensively studied in CAD. This study confirmed the differential expression of both miRNAs in the control and patient samples using qRT-PCR. The current study also tried to put forward a strategy to quantify the miRNAs in disease and control samples by measuring fluorescence intensity. We also elucidated the expression of several proteins involved in apoptotic signaling pathways and confirmed the miR-98-5p targets by using miRNA mimic.

In the current study ISO was used for the establishment of the MI rat model and performed biochemical assays for confirmation of the disease model. HW/BW and HW/TL were assessed as an index of MI. An increase in these ratios was observed in the case of ISO rats suggesting cardiovascular disease conditions. This increase in HW/BW and HW/TL ratios was in accordance with previous studies where they have been linked to cardiac hypertrophy and MI conditions (Ali et al., 2019; Feng et al., 2019).

To validate oxidative stress, we performed oxidants and antioxidant profiling using the blood and heart tissue of rats. The ROS levels and TBARs depicted the presence of oxidative species in cells and the lipid peroxidation products levels respectively in tissues. We found the levels of both ROS and TBARs to be elevated in both blood and heart tissue of ISO group suggesting increased ROS leading to the oxidized lipid accumulation in the tissues. The oxidative stress was further validated by investigating the activities of antioxidant enzymes in both heart and tissue samples. SOD is the primary defense against oxidants (Ighodaro & Akinloye, 2018). The level of SOD

activity was found to be downregulated in the ISO group. CAT and GSH catalyze the conversion of  $H_2O_2$  to  $H_2O$ . The activity of CAT and GSH were found to be downregulated in case of ISO group suggesting an increased  $H_2O_2$  accumulation in the tissues. Moreover, APX and POD also catalyze the conversion of ROS into less toxic metabolites (Sharma, Jha, Dubey, & Pessarakli, 2012). The activity levels of APX and POD were found to be significantly downregulated in the diseased group. Overall, a marked decline in the activities of antioxidant enzymes was observed in ISO group and the level of ROS was found to be elevated that eventually lead to the oxidative stress and lipid peroxidation in the cells. Previously, several studies showed role of increased oxidative stress during cardiovascular and cardiometabolic pathologies (Cervantes Gracia, Llanas-Cornejo, & Husi, 2017; Singh & Jialal, 2006).

ISO induction is reported to cause the changes in lipid metabolism (Khan, Sharma, Bhandari, Ali, & Haque, 2018). To assess changes in lipid metabolism, lipid profiling was done by assessing levels of triglycerides and cholesterol. A significant elevation in the triglycerides and cholesterol levels in the blood of the ISO group. This finding is in accordance with the previously reported study that suggests that ISO-induced rats have increased lipid biosynthesis and decreased fatty acid oxidation resulting in increased triglycerides and cholesterol levels (Mehmet et al., 2022). Moreover, hyperlipidemia and hypercholesterolemia are risk factors for CVDs and hence confirmed diseased model.

Liver injury markers including ALT and AST were also assessed. The levels of ALT and AST activities were elevated in ISO treated rat's group. It has previously been reported that patients with acute or chronic heart failure conditions have an elevated level of liver enzymes (Al-U'datt et al., 2023). In our studies, elevated levels of ALT and AST enzyme activities suggest a cardiac hepatic relationship and confirm the disease model establishment.

For elucidating the diagnostic role of miRNAs in CAD, the circulatory levels of miRNAs were assessed. Our results demonstrated that the circulatory levels of miR-1-3p were remarkably increased in the CAD patient's blood in contrast to the control individuals. This suggests the role of miR-1-3p as a putative diagnostic biomarker for CAD. Previously, miR-1-3p is reported to have roles in angiogenesis, and cardiogenesis (Kaur et al., 2019). The plasma level of miR-1-3p is reported to be elevated in

MI (Li, Dong, Wang, & Wu, 2014). We also assessed the circulatory levels of miR-98-5p, and it was found that the circulatory level of this miRNA was significantly downregulated in CAD in contrast to controls. Previously, miR-98-5p is reported to be involved in endothelial dysfunction and in cerebrovascular diseases (Tong, Tan, Lim, Tien, & Wong, 2022; Zheng, Zhang, Liang, & Li, 2021). Consistent results were found in the case of ISO and control rat groups, with a decreased level of miR-98-5p in the whole blood and heart tissue of ISO rats. Moreover, the tissue levels of miR-1-3p were found to be diminished as reported previously in the autopsy samples of MI hearts (Boštjančič, Zidar, Štajer, & Glavač, 2009). This suggested that ISO has induced MI in rats subsequently changing the miRNA levels in contrast to normal controls.

To further confirm the diagnostic potential of miRNA-1-3p, we quantified the miRNA-1-3p in blood samples of controls and CAD patients using a fluorometer. The fluorescence intensity of miR-1-3p was increased in CAD patients suggesting a higher quantity of miR-1-3p in CAD patients. Previously, no study has been reported to quantify miRNAs by measuring the fluorescence intensity. Thus, we attempted to provide a novel strategy to quantify miRNAs in human whole blood samples.

The miRNAs play the role in disease etiology by targeting the different mRNAs. So, to confirm the role of miRNAs in CAD, the mRNA expression levels of the target genes NFATc3, ET-1, Bcl-2, and BAX was assessed in whole blood samples of humans and rats. In circulation, miRNAs are present in various forms including exosomal vesicles, or bound to AGO2 proteins (O'Brien, Hayder, Zayed, & Peng, 2018). Dysregulated expression of miRNAs in blood results in the dysregulation of their target genes' mRNA levels. Herein, we assessed the circulatory mRNA level expression of NFATc3 and Et-1 in control and disease group. NFATc3 levels were observed to be significantly downregulated in the blood samples of both ISO-rats and CAD patients. This result supports the finding that NFATc3 can prevent foam cell formation in macrophages (Liu et al., 2021). None of the previous studies reported NFATc3 levels in the whole blood. ET-1 showed increased relative expression in the whole blood of ISO-treated rats as well as in CAD patients suggesting endothelial dysfunction in CAD leading to MI. ET-1 levels were previously reported to be elevated in serum samples of CAD patients in comparison to control population (Lin et al., 2023) and in diseased rats (Fan et al., 2020). The relative expression of Bcl-2 and BAX were also assessed as a marker of apoptosis. Bcl-2-an antiapoptotic protein-is found to be downregulated in CAD patients

and ISO rats. BAX showed an elevated expression in the whole blood of CAD patients and ISO group. Increased expression of BAX and downregulation of Bcl-2 depicted increased apoptosis in these groups that is also linked to MI and CAD in various previous studies (Mohammadi et al., 2021).

Moreover, we also assessed the expression of miRNAs and mRNA expression level of genes in the heart tissues of rats. The levels of miR-98-5p were observed to be decreased in ISO treated rats. On the contrary to circulatory levels of miR-1-3p, its level was found to be reduced in the heart tissue. Moreover, the levels of NFATc3, BAX, Bcl-2, and ET-1 were also assessed. A significant upregulation of NFATc3, ET-1, and BAX was observed in the ISO-induced rats while a remarkably reduced expression of Bcl-2 was observed in the case of diseased rat heart tissue. Increased level of NFATc3 suggests cardiac hypertrophic development. No previous study has reported mRNA level of NFATc3 in the heart tissue of rats. Increased ET-1 suggests endothelial dysfunction and increased ROS accumulation in the cardiomyocytes causing CAD development and eventually leading to MI. Previously ET-1 levels are reported to be elevated in ISO-induced rats (Aliska, Katar, Endo Mahata, Pratiwi, & Nuranisyah, 2022). Moreover, a disrupted BAX/ Bcl-2 ratio in favor of BAX suggests apoptosis in the cardiac cells that promote MI as reported previously (Abukhalil et al., 2021).

For validating the targets genes of miR-98-5p, western blotting was also performed. Increased expression of ET-1 protein was observed in ISO group in contrast to the control. After miR-98-5p mimic administration, a reduction in the protein expression of ET-1 was observed. This confirms ET-1 as the main target of miR-98-5p. As ET-1 is involved in endothelial dysfunction, oxidative stress, cardiac hypertrophic conditions, mitochondrial damage, and apoptosis, its downstream modulators including NFATc3, Drp-1, and BAX were also assessed. NFATc3 levels were elevated in the diseased group in comparison to the control group suggesting cardiac hypertrophic events. Rats having miR-98-5p mimic dose have shown a decreased expression of NFATc3 indicating the role of miR-98-5p in controlling cardiac hypertrophy development. Moreover, concomitant dosing of miR-98-5p mimic and ISO to the rats have also shown a substantial decrease in the protein expression level of BAX and Drp-1 suggesting a reduction in mitochondrial apoptotic pathways within these diseased rats. No previous study has reported the impact of miR-98-5p mimic dosage on protein expression in ISO-induced MI rats.

Conclusively, various risk factors result in ROS accumulation in the cells which has several consequences. Increased ROS causes oxidation of LDL in the cells, decreased production of NO, and increased production of Et-1 which eventually results in endothelial dysfunction (Crea, Montone, & Rinaldi, 2022). Our study suggested a link between miRNA expression and CAD development. Increased levels of miR-1-3p in blood resulted in the decreased NFATc3 level so it can't be able to transcribe miR-204 and prevent foam cell formation as reported previously. Decreased level of miR-98-5p caused an elevation in ET-1, in both blood cells and cardiac muscle cells, promoted the endothelial dysfunction and NO degradation, hence promoting vasoconstriction. The dysfunctional endothelium has an increased expression of cell adhesion molecules (V-CAM, I-CAM), monocyte adhesion molecules, E-selectin and P-selection that promote platelet and monocytes adhesion and engulfment (Melo et al., 2004). These monocytes with an increased Et-1 and decreased NFATc3 eventually develop foam cells and differentiate into macrophages in the presence of oxidative stress and oxidized-LDL. This increased oxidative stress also results in mitochondrial dysfunction leading to the opening of the mitochondrial membrane permeability channels resulting in the  $Ca^{+2}$  release in the cytosol. Increased  $Ca^{+2}$  levels result in activation of calcium-calmodulin phosphatase that dephosphorylates NFATc3 and allows its nuclear localization. Moreover, in contrast to the circulatory levels of miR-1-3p the tissue levels of this miRNA were found to be downregulated that resulted in the increase in NFATc3 levels. Increased NFATc3 hence will promote the cardiac hypertrophic genes expression and NOX hence promoting oxidative stress (P. Zhang et al., 2023). NOX disrupts the BAX/Bcl ratio favoring apoptosis (P. Zhang et al., 2023). The presence of ox-LDL and increased ET-1 will cause the increased expression of LOX-1 receptor that will promote the apoptosis by downregulating the antioxidant Bcl-2 and increasing cytochrome-c release (J. Chen et al., 2004; D. Li & Mehta, 2009). Calcineurin also dephosphorylates DRP-1 and activates it. Activation of DRP-1 allows the VSMC proliferation and migration and mitochondrial fission process (Rogers et al., 2017). This recruitment of Drp-1 facilitates the recruitment of BAX and hence promote mitochondrial fission associated apoptosis (Maes, Grosser, Fehrman, Schlamp, & Nickells, 2019). Our study elucidated the interplay of apoptotic pathways and miRNAs expression for CAD development and confirmation of target genes by using miR-98-5p mimics. To the best of our knowledge, no previous study has reported miRNAs as the biomarkers of CVDs. Keeping in view the differential expression of miRNAs in CAD patients, this study put



forward the miRNA-1-3p and miR-98-5p as the potential diagnostic biomarkers for CAD. However, further clinical trials are required to develop these miRNAs as diagnostic biomarkers that may open up new avenues of research for better disease diagnosis and management.

## 5. REFERENCES

- Al-U'datt, D. a. G. F., Tranchant, C. C., Alu'datt, M., Abusara, S., Al-Dwairi, A., AlQudah, M., . . . Alzoubi, K. H. (2023). Inhibition of transglutaminase 2 (TG2) ameliorates ventricular fibrosis in isoproterenol-induced heart failure in rats. *Life Sciences*, 321, 121564. doi:<https://doi.org/10.1016/j.lfs.2023.121564>
- Ali, T., Mushtaq, I., Maryam, S., Farhan, A., Saba, K., Jan, M. I., . . . Hamera, S. (2019). Interplay of N acetyl cysteine and melatonin in regulating oxidative stress-induced cardiac hypertrophic factors and microRNAs. *Archives of biochemistry and biophysics*, 661, 56-65.
- Aliska, G., Katar, Y., Endo Mahata, L., Pratiwi, N., & Nuranisyah, V. (2022). Effect of Ramipril on Endothelin-1 Expression in Myocardial Tissue at Wistar Rats Induced Myocardial Infarction. *Open Access Macedonian Journal of Medical Sciences*, 10(A), 33-37. doi:[10.3889/oamjms.2022.7676](https://doi.org/10.3889/oamjms.2022.7676)
- Cervantes Gracia, K., Llanas-Cornejo, D., & Husi, H. (2017). CVD and Oxidative Stress. *Journal of Clinical Medicine*, 6(2), 22.
- Fan, S., Zhang, J., Xiao, Q., Liu, P., Zhang, Y., Yao, E., & Chen, X. (2020). Cardioprotective effect of the polysaccharide from *Ophiopogon japonicus* on isoproterenol-induced myocardial ischemia in rats. *International Journal of Biological Macromolecules*, 147, 233-240. doi:<https://doi.org/10.1016/j.ijbiomac.2020.01.068>
- Feng, L., Ren, J., Li, Y., Yang, G., Kang, L., Zhang, S., . . . Qi, Z. (2019). Resveratrol protects against isoproterenol induced myocardial infarction in rats through VEGF-B/AMPK/eNOS/NO signalling pathway. *Free Radical Research*, 53(1), 82-93. doi:[10.1080/10715762.2018.1554901](https://doi.org/10.1080/10715762.2018.1554901)
- Ighodaro, O. M., & Akinloye, O. A. (2018). First line defence antioxidants-superoxide dismutase (SOD), catalase (CAT) and glutathione peroxidase (GPX): Their fundamental role in the entire antioxidant defence grid. *Alexandria Journal of Medicine*, 54(4), 287-293. doi:[10.1016/j.ajme.2017.09.001](https://doi.org/10.1016/j.ajme.2017.09.001)
- Kaur, A., Mackin, S. T., Schlosser, K., Wong, F. L., Elharram, M., Delles, C., . . . Pilote, L. (2019). Systematic review of microRNA biomarkers in acute coronary syndrome and stable coronary artery disease. *Cardiovascular Research*, 116(6), 1113-1124. doi:[10.1093/cvr/cvz302](https://doi.org/10.1093/cvr/cvz302)
- Khan, V., Sharma, S., Bhandari, U., Ali, S. M., & Haque, S. E. (2018). Raspberry ketone protects against isoproterenol-induced myocardial infarction in rats. *Life Sciences*, 194, 205-212. doi:<https://doi.org/10.1016/j.lfs.2017.12.013>
- Li, J., Dong, X., Wang, Z., & Wu, J. (2014). MicroRNA-1 in cardiac diseases and cancers. *The Korean Journal of Physiology & Pharmacology: Official Journal of the Korean Physiological Society and the Korean Society of Pharmacology*, 18(5), 359.
- Lin, R., Junntila, J., Piuholta, J., Lepojärvi, E. S., Magga, J., Kiviniemi, A. M., . . . Kerkelä, R. (2023). Endothelin-1 is associated with mortality that can be attenuated with high intensity statin therapy in patients with stable coronary artery disease. *Communications Medicine*, 3(1), 87. doi:[10.1038/s43856-023-00322-9](https://doi.org/10.1038/s43856-023-00322-9)
- Liu, X., Guo, J.-W., Lin, X.-C., Tuo, Y.-H., Peng, W.-L., He, S.-Y., . . . Liang, S.-J. (2021). Macrophage NFATc3 prevents foam cell formation and atherosclerosis: evidence and mechanisms. *European Heart Journal*, 42(47), 4847-4861. doi:[10.1093/eurheartj/ehab660](https://doi.org/10.1093/eurheartj/ehab660)
- Mehmet, E., Güngör, H., Karayığıt, M. Ö., Turgut, N. H., Koçkaya, M., Karataş, Ö., & Üner, A. G. (2022). Cardioprotective Effect of Empagliflozin in Rats with

- Isoproterenol-Induced Myocardial Infarction: Evaluation of Lipid Profile, Oxidative Stress, Inflammation, DNA Damage, and Apoptosis. *Biology Bulletin*, 49(1), S159-S172. doi:10.1134/S1062359022130039
- Mohammadi, A., Balizadeh Karami, A. R., Dehghan Mashtani, V., Sahraei, T., Bandani Tarashoki, Z., Khattavian, E., . . . Radmanesh, E. (2021). Evaluation of Oxidative Stress, Apoptosis, and Expression of MicroRNA-208a and MicroRNA-1 in Cardiovascular Patients. *Rep Biochem Mol Biol*, 10(2), 183-196. doi:10.52547/rbmb.10.2.183
- O'Brien, J., Hayder, H., Zayed, Y., & Peng, C. (2018). Overview of microRNA biogenesis, mechanisms of actions, and circulation. *Frontiers in endocrinology*, 9, 402.
- Prince, P. S. M., Dhanasekar, K., & Rajakumar, S. (2011). Preventive Effects of Vanillic Acid on Lipids, Bax, Bcl-2 and Myocardial Infarct Size on Isoproterenol-Induced Myocardial Infarcted Rats: A Biochemical and In Vitro Study. *Cardiovascular Toxicology*, 11(1), 58-66. doi:10.1007/s12012-010-9098-3
- Sharma, P., Jha, A. B., Dubey, R. S., & Pessarakli, M. (2012). Reactive oxygen species, oxidative damage, and antioxidative defense mechanism in plants under stressful conditions. *Journal of botany*, 2012.
- Sheikh, S. A. (2020). Role of plasma soluble lectin like oxidized low-density lipoprotein receptor-1 in severity of CAD patients and relationship with microRNA-98. *Med. J.*
- Singh, U., & Jialal, I. (2006). Oxidative stress and atherosclerosis. *Pathophysiology*, 13(3), 129-142. doi:https://doi.org/10.1016/j.pathophys.2006.05.002
- Tong, K.-L., Tan, K.-E., Lim, Y.-Y., Tien, X.-Y., & Wong, P.-F. (2022). CircRNA-miRNA interactions in atherogenesis. *Molecular and Cellular Biochemistry*, 477(12), 2703-2733. doi:10.1007/s11010-022-04455-8
- Zheng, Z., Zhang, G., Liang, X., & Li, T. (2021). LncRNA OIP5-AS1 facilitates ox-LDL-induced endothelial cell injury through the miR-98-5p/HMGB1 axis. *Molecular and Cellular Biochemistry*, 476(1), 443-455. doi:10.1007/s11010-020-03921-5
- Abukhalil, M. H., Hussein, O. E., Aladaileh, S. H., Althunibat, O. Y., Al-Amarat, W., Saghir, S. A., . . . Mahmoud, A. M. (2021). Visnagin prevents isoproterenol-induced myocardial injury by attenuating oxidative stress and inflammation and upregulating Nrf2 signaling in rats. *Journal of Biochemical and Molecular Toxicology*, 35(11), e22906. doi:<https://doi.org/10.1002/jbt.22906>
- Acuña, S. M., Floeter-Winter, L. M., & Muxel, S. M. (2020). MicroRNAs: Biological Regulators in Pathogen-Host Interactions. *Cells*, 9(1), 113.
- Ali Sheikh, M. S., Alduraywish, A., Almaeen, A., Alruwali, M., Alruwaili, R., Alomair, B. M., . . . A.M.Abdulhabeeb, I. (2021). Therapeutic Value of miRNAs in Coronary Artery Disease. *Oxid Med Cell Longev*, 2021, 8853748. doi:10.1155/2021/8853748
- Ali, T., Shaheen, F., Mahmud, M., Waheed, H., Jan, M. I., Javed, Q., & Murtaza, I. (2015). Serotonin-promoted elevation of ROS levels may lead to cardiac pathologies in diabetic rat. *Arch Biol Sci*, 67(2), 655-661.
- Ali, T., Waheed, H., Shaheen, F., Mahmud, M., Javed, Q., & Murtaza, I. (2015). Increased endogenous serotonin level in diabetic conditions may lead to cardiac valvulopathy via reactive oxygen species regulation. *Biologia*, 70(2), 273-278.
- Álvarez-Álvarez, M. M., Zanetti, D., Carreras-Torres, R., Moral, P., & Athanasiadis, G. (2017). A survey of sub-Saharan gene flow into the Mediterranean at risk loci for coronary artery disease. *European Journal of Human Genetics*, 25(4), 472-476.

- Badacz, R., Kleczyński, P., Legutko, J., Żmudka, K., Gacoń, J., Przewłocki, T., & Kabłak-Ziembicka, A. (2021). Expression of miR-1-3p, miR-16-5p and miR-122-5p as Possible Risk Factors of Secondary Cardiovascular Events. *Biomedicines*, *9*(8), 1055.
- Basatemur, G. L., Jørgensen, H. F., Clarke, M. C. H., Bennett, M. R., & Mallat, Z. (2019). Vascular smooth muscle cells in atherosclerosis. *Nature Reviews Cardiology*, *16*(12), 727-744. doi:10.1038/s41569-019-0227-9
- Björkegren, J. L. M., & Lusis, A. J. (2022). Atherosclerosis: Recent developments. *Cell*, *185*(10), 1630-1645. doi:10.1016/j.cell.2022.04.004
- Böhm, F., & Pernow, J. (2007). The importance of endothelin-1 for vascular dysfunction in cardiovascular disease. *Cardiovascular Research*, *76*(1), 8-18. doi:10.1016/j.cardiores.2007.06.004
- Boštjančič, E., Zidar, N., Štajer, D., & Glavač, D. (2009). MicroRNAs miR-1, miR-133a, miR-133b and miR-208 Are Dysregulated in Human Myocardial Infarction. *Cardiology*, *115*(3), 163-169. doi:10.1159/000268088
- Cai, Y., Yao, H., Sun, Z., Wang, Y., Zhao, Y., Wang, Z., & Li, L. (2021). Role of NFAT in the Progression of Diabetic Atherosclerosis. *Frontiers in Cardiovascular Medicine*, *8*. doi:10.3389/fcvm.2021.635172
- Chen, J., Mehta, J. L., Haider, N., Zhang, X., Narula, J., & Li, D. (2004). Role of Caspases in Ox-LDL-Induced Apoptotic Cascade in Human Coronary Artery Endothelial Cells. *Circulation Research*, *94*(3), 370-376. doi:10.1161/01.RES.0000113782.07824.BE
- Chen, X., Zhang, L., Su, T., Li, H., Huang, Q., Wu, D., . . . Han, Z. (2015). Kinetics of plasma microRNA-499 expression in acute myocardial infarction. *Journal of thoracic disease*, *7*(5), 890.
- Chiong, M., Wang, Z. V., Pedrozo, Z., Cao, D. J., Troncoso, R., Ibacache, M., . . . Lavandero, S. (2011). Cardiomyocyte death: mechanisms and translational implications. *Cell Death & Disease*, *2*(12), e244-e244. doi:10.1038/cddis.2011.130
- Crea, F., Montone, R. A., & Rinaldi, R. (2022). Pathophysiology of coronary microvascular dysfunction. *Circulation Journal*, *86*(9), 1319-1328.
- Daiber, A., Hahad, O., Andreadou, I., Steven, S., Daub, S., & Münzel, T. (2021). Redox-related biomarkers in human cardiovascular disease - classical footprints and beyond. *Redox Biology*, *42*, 101875. doi:<https://doi.org/10.1016/j.redox.2021.101875>
- Ellis, B. W., Ronan, G., Ren, X., Bahcecioglu, G., Senapati, S., Anderson, D., . . . Zorlutuna, P. (2022). Human Heart Anoxia and Reperfusion Tissue (HEART) Model for the Rapid Study of Exosome Bound miRNA Expression As Biomarkers for Myocardial Infarction. *Small*, *18*(28), 2201330. doi:<https://doi.org/10.1002/sml.202201330>
- Fialkow, L., Wang, Y., & Downey, G. P. (2007). Reactive oxygen and nitrogen species as signaling molecules regulating neutrophil function. *Free radical biology and medicine*, *42*(2), 153-164. doi:<https://doi.org/10.1016/j.freeradbiomed.2006.09.030>
- Förstermann, U., Closs, E. I., Pollock, J. S., Nakane, M., Schwarz, P., Gath, I., & Kleinert, H. (1994). Nitric oxide synthase isozymes. Characterization, purification, molecular cloning, and functions. *Hypertension*, *23*(6\_pt\_2), 1121-1131. doi:10.1161/01.HYP.23.6.1121
- Förstermann, U., & Münzel, T. (2006). Endothelial Nitric Oxide Synthase in Vascular Disease. *Circulation*, *113*(13), 1708-1714. doi:10.1161/CIRCULATIONAHA.105.602532
- Gebert, L. F., & MacRae, I. J. (2019). Regulation of microRNA function in animals. *Nature reviews Molecular cell biology*, *20*(1), 21-37.
- Gebert, L. F. R., & MacRae, I. J. (2019). Regulation of microRNA function in animals. *Nature reviews Molecular cell biology*, *20*(1), 21-37. doi:10.1038/s41580-018-0045-7
- Gholaminejad, A., Zare, N., Dana, N., Shafie, D., Mani, A., & Javanmard, S. H. (2021). A meta-analysis of microRNA expression profiling studies in heart failure. *Heart Failure Reviews*, *26*(4), 997-1021. doi:10.1007/s10741-020-10071-9

- Gianazza, E., Brioschi, M., Fernandez, A. M., & Banfi, C. (2019). Lipoxidation in cardiovascular diseases. *Redox Biology*, 23, 101119. doi:<https://doi.org/10.1016/j.redox.2019.101119>
- Gonzalez, L., & Trigatti, B. L. (2017). Macrophage apoptosis and necrotic core development in atherosclerosis: a rapidly advancing field with clinical relevance to imaging and therapy. *Canadian Journal of Cardiology*, 33(3), 303-312.
- Graham, I., Atar, D., Borch-Johnsen, K., Boysen, G., Burell, G., Cifkova, R., . . . Gjelsvik, B. (2007). European guidelines on cardiovascular disease prevention in clinical practice: executive summary: Fourth Joint Task Force of the European Society of Cardiology and Other Societies on Cardiovascular Disease Prevention in Clinical Practice (Constituted by representatives of nine societies and by invited experts). *European heart journal*, 28(19), 2375-2414.
- Ha, M., & Kim, V. N. (2014). Regulation of microRNA biogenesis. *Nature reviews Molecular cell biology*, 15(8), 509-524. doi:10.1038/nrm3838
- Harada, M., Luo, X., Murohara, T., Yang, B., Dobrev, D., & Nattel, S. (2014). MicroRNA Regulation and Cardiac Calcium Signaling. *Circulation Research*, 114(4), 689-705. doi:doi:10.1161/CIRCRESAHA.114.301798
- Hayashi, I., Morishita, Y., Imai, K., Nakamura, M., Nakachi, K., & Hayashi, T. (2007). High-throughput spectrophotometric assay of reactive oxygen species in serum. *Mutation Research/Genetic Toxicology and Environmental Mutagenesis*, 631(1), 55-61. doi:<https://doi.org/10.1016/j.mrgentox.2007.04.006>
- He, L., He, T., Farrar, S., Ji, L., Liu, T., & Ma, X. (2017). Antioxidants Maintain Cellular Redox Homeostasis by Elimination of Reactive Oxygen Species. *Cellular Physiology and Biochemistry*, 44(2), 532-553. doi:10.1159/000485089
- Hosseini, A., Rajabian, A., Sobhanifar, M.-A., Alavi, M. S., Taghipour, Z., Hasanpour, M., . . . Sahebkar, A. (2022). Attenuation of isoprenaline-induced myocardial infarction by *Rheum turkestanicum*. *Biomedicine & Pharmacotherapy*, 148, 112775. doi:<https://doi.org/10.1016/j.biopha.2022.112775>
- Incalza, M. A., D'Oria, R., Natalicchio, A., Perrini, S., Laviola, L., & Giorgino, F. (2018). Oxidative stress and reactive oxygen species in endothelial dysfunction associated with cardiovascular and metabolic diseases. *Vascular pharmacology*, 100, 1-19.
- Ishtiaq, A., Bakhtiar, A., Silas, E., Saeed, J., Ajmal, S., Mushtaq, I., . . . Murtaza, I. (2020). Pistacia integerrima alleviated Bisphenol A induced toxicity through Ubc13/p53 signalling. *Molecular Biology Reports*, 47(9), 6545-6559. doi:10.1007/s11033-020-05706-x
- Jan, M. I., Khan, R. A., Ali, T., Bilal, M., Bo, L., Sajid, A., . . . Nawab, J. (2017). Interplay of mitochondria apoptosis regulatory factors and microRNAs in valvular heart disease. *Archives of biochemistry and biophysics*, 633, 50-57.
- Janota, T. (2014). Biochemical markers in the diagnosis of myocardial infarction. *Cor et Vasa*, 56(4), e304-e310. doi:<https://doi.org/10.1016/j.crvasa.2014.06.007>
- Jollow, D., Mitchell, J., Zampaglione, N. a., & Gillette, J. (1974). Bromobenzene-induced liver necrosis. Protective role of glutathione and evidence for 3, 4-bromobenzene oxide as the hepatotoxic metabolite. *Pharmacology*, 11(3), 151-169.
- Kang, B.-Y., Park, K. K., Kleinhenz, J. M., Murphy, T. C., Green, D. E., Bijli, K. M., . . . Hart, C. M. (2016). Peroxisome Proliferator-Activated Receptor  $\gamma$  and microRNA 98 in Hypoxia-Induced Endothelin-1 Signaling. *American Journal of Respiratory Cell and Molecular Biology*, 54(1), 136-146. doi:10.1165/rcmb.2014-0337OC
- Karbowski, M., Lee, Y.-J., Gaume, B., Jeong, S.-Y., Frank, S., Nechushtan, A., . . . Youle, R. J. (2002). Spatial and temporal association of Bax with mitochondrial fission sites, Drp1, and Mfn2 during apoptosis. *The Journal of cell biology*, 159(6), 931-938.
- Korshunova, A. Y., Blagonravov, M. L., Neborak, E. V., Syatkin, S. P., Sklifasovskaya, A. P., Semyatov, S. M., & Agostinelli, E. (2021). BCL2-regulated apoptotic process in

- myocardial ischemia-reperfusion injury (Review). *Int J Mol Med*, 47(1), 23-36. doi:10.3892/ijmm.2020.4781
- Kosuge, M., Kimura, K., Ishikawa, T., Ebina, T., Hibi, K., Tsukahara, K., . . . Nozawa, N. (2006). Differences between men and women in terms of clinical features of ST-segment elevation acute myocardial infarction. *Circulation Journal*, 70(3), 222-226.
- Leitão, A. L., & Enguita, F. J. (2022). A Structural View of miRNA Biogenesis and Function. *Non-Coding RNA*, 8(1), 10.
- Li, D., & Mehta, J. L. (2009). Intracellular Signaling of LOX-1 in Endothelial Cell Apoptosis. *Circulation Research*, 104(5), 566-568. doi:doi:10.1161/CIRCRESAHA.109.194209
- Li, L. M., Cai, W. B., Ye, Q., Liu, J. M., Li, X., & Liao, X. X. (2014). Comparison of plasma microRNA-1 and cardiac troponin T in early diagnosis of patients with acute myocardial infarction. *World J Emerg Med*, 5(3), 182-186. doi:10.5847/wjem.j.issn.1920-8642.2014.03.004
- Libby, P. (2021). The changing landscape of atherosclerosis. *Nature*, 592(7855), 524-533.
- Liochev, S. I. (2013). Reactive oxygen species and the free radical theory of aging. *Free radical biology and medicine*, 60, 1-4.
- Liu, X., Guo, J.-W., Lin, X.-C., Tuo, Y.-H., Peng, W.-L., He, S.-Y., . . . Liang, S.-J. (2021). Macrophage NFATc3 prevents foam cell formation and atherosclerosis: evidence and mechanisms. *European heart journal*, 42(47), 4847-4861. doi:10.1093/eurheartj/ehab660
- Lobo Filho, H. G., Ferreira, N. L., Sousa, R. B. d., Carvalho, E. R. d., Lobo, P. L. D., & Lobo Filho, J. G. (2011). Experimental model of myocardial infarction induced by isoproterenol in rats. *Brazilian Journal of Cardiovascular Surgery*, 26, 469-476.
- Maes, M. E., Grosser, J. A., Fehrman, R. L., Schlamp, C. L., & Nickells, R. W. (2019). Completion of BAX recruitment correlates with mitochondrial fission during apoptosis. *Scientific Reports*, 9(1), 16565. doi:10.1038/s41598-019-53049-w
- Malakar, A. K., Choudhury, D., Halder, B., Paul, P., Uddin, A., & Chakraborty, S. (2019). A review on coronary artery disease, its risk factors, and therapeutics. *Journal of Cellular Physiology*, 234(10), 16812-16823. doi:<https://doi.org/10.1002/jcp.28350>
- Martinet, W., Schrijvers, D. M., & De Meyer, G. R. Y. (2011). Necrotic cell death in atherosclerosis. *Basic Research in Cardiology*, 106(5), 749-760. doi:10.1007/s00395-011-0192-x
- Matsuyama, H., & Suzuki, H. I. (2020). Systems and Synthetic microRNA Biology: From Biogenesis to Disease Pathogenesis. *International Journal of Molecular Sciences*, 21(1), 132.
- Medina-Leyte, D. J., Zepeda-García, O., Domínguez-Pérez, M., González-Garrido, A., Villarreal-Molina, T., & Jacobo-Albavera, L. (2021). Endothelial Dysfunction, Inflammation and Coronary Artery Disease: Potential Biomarkers and Promising Therapeutical Approaches. *International Journal of Molecular Sciences*, 22(8), 3850.
- Melak, T., & Baynes, H. W. (2019). Circulating microRNAs as possible biomarkers for coronary artery disease: a narrative review. *Ejifcc*, 30(2), 179-194.
- Melo, L. G., Gneccchi, M., Pachori, A. S., Kong, D., Wang, K., Liu, X., . . . Dzau, V. J. (2004). Endothelium-Targeted Gene and Cell-Based Therapies for Cardiovascular Disease. *Arteriosclerosis, Thrombosis, and Vascular Biology*, 24(10), 1761-1774. doi:doi:10.1161/01.ATV.0000142363.15113.88
- Mohan Manu, T., Anand, T., Sharath Babu, G., Patil, M. M., & Khanum, F. (2022). Bacopa monniera extract mitigates isoproterenol-induced cardiac stress via Nrf2/Keap1/NQO1 mediated pathway. *Archives of Physiology and Biochemistry*, 128(2), 341-351.
- Mori, H., Torii, S., Kutyna, M., Sakamoto, A., Finn, A. V., & Virmani, R. (2018). Coronary Artery Calcification and its Progression: What Does it Really Mean? *JACC: Cardiovascular Imaging*, 11(1), 127-142. doi:<https://doi.org/10.1016/j.jcmg.2017.10.012>

- Mundi, S., Massaro, M., Scoditti, E., Carluccio, M. A., van Hinsbergh, V. W. M., Iruela-Arispe, M. L., & De Caterina, R. (2017). Endothelial permeability, LDL deposition, and cardiovascular risk factors—a review. *Cardiovascular Research*, *114*(1), 35-52. doi:10.1093/cvr/cvx226
- Muniyappa, R., Chen, H., Montagnani, M., Sherman, A., & Quon, M. J. (2020). Endothelial dysfunction due to selective insulin resistance in vascular endothelium: insights from mechanistic modeling. *American Journal of Physiology-Endocrinology and Metabolism*, *319*(3), E629-E646. doi:10.1152/ajpendo.00247.2020
- Murphy, E., & Liu, J. C. (2022). Mitochondrial calcium and reactive oxygen species in cardiovascular disease. *Cardiovascular Research*, cvac134.
- Naeli, P., Winter, T., Hackett, A. P., Alboushi, L., & Jafarnejad, S. M. The intricate balance between microRNA-induced mRNA decay and translational repression. *The FEBS Journal*, n/a(n/a). doi:<https://doi.org/10.1111/febs.16422>
- Nakano, Y., & Asada, K. (1981). Hydrogen Peroxide is Scavenged by Ascorbate-specific Peroxidase in Spinach Chloroplasts. *Plant and Cell Physiology*, *22*(5), 867-880. doi:10.1093/oxfordjournals.pcp.a076232
- Navickas, R., Gal, D., Laucevičius, A., Taparuskaitė, A., Zdanytė, M., & Holvoet, P. (2016). Identifying circulating microRNAs as biomarkers of cardiovascular disease: a systematic review. *Cardiovascular Research*, *111*(4), 322-337. doi:10.1093/cvr/cvw174
- Pacher, P., Beckman, J. S., & Liaudet, L. (2007). Nitric Oxide and Peroxynitrite in Health and Disease. *Physiological Reviews*, *87*(1), 315-424. doi:10.1152/physrev.00029.2006
- Pagan, L. U., Gomes, M. J., Gatto, M., Mota, G. A. F., Okoshi, K., & Okoshi, M. P. (2022). The Role of Oxidative Stress in the Aging Heart. *Antioxidants*, *11*(2), 336.
- Park, M. S., Phan, H.-D., Busch, F., Hinckley, S. H., Brackbill, J. A., Wysocki, V. H., & Nakanishi, K. (2017). Human Argonaute3 has slicer activity. *Nucleic acids research*, *45*(20), 11867-11877.
- Parra, V., Eisner, V., Chiong, M., Criollo, A., Moraga, F., Garcia, A., . . . Hidalgo, C. (2008). Changes in mitochondrial dynamics during ceramide-induced cardiomyocyte early apoptosis. *Cardiovascular Research*, *77*(2), 387-397.
- Rajadurai, M., & Stanely Mainzen Prince, P. (2007). Preventive effect of naringin on cardiac markers, electrocardiographic patterns and lysosomal hydrolases in normal and isoproterenol-induced myocardial infarction in Wistar rats. *Toxicology*, *230*(2), 178-188. doi:<https://doi.org/10.1016/j.tox.2006.11.053>
- Rogers, M. A., Maldonado, N., Hutcheson, J. D., Goettsch, C., Goto, S., Yamada, I., . . . Aikawa, E. (2017). Dynamin-Related Protein 1 Inhibition Attenuates Cardiovascular Calcification in the Presence of Oxidative Stress. *Circ Res*, *121*(3), 220-233. doi:10.1161/circresaha.116.310293
- Rotariu, D., Babes, E. E., Tit, D. M., Moisi, M., Bustea, C., Stoicescu, M., . . . Bungau, S. G. (2022). Oxidative stress – Complex pathological issues concerning the hallmark of cardiovascular and metabolic disorders. *Biomedicine & Pharmacotherapy*, *152*, 113238. doi:<https://doi.org/10.1016/j.biopha.2022.113238>
- Senoner, T., & Dichtl, W. (2019). Oxidative Stress in Cardiovascular Diseases: Still a Therapeutic Target? *Nutrients*, *11*(9). doi:10.3390/nu11092090
- Shankar, K., & Mehendale, H. M. (2014). Oxidative Stress. In P. Wexler (Ed.), *Encyclopedia of Toxicology (Third Edition)* (pp. 735-737). Oxford: Academic Press.
- Sheikh, S. A. (2020). Role of plasma soluble lectin like oxidized low-density lipoprotein receptor-1 in severity of CAD patients and relationship with microRNA-98. *Med. J.*
- Solaro, C. R., & Solaro, R. J. (2020). Implications of the complex biology and micro-environment of cardiac sarcomeres in the use of high affinity troponin antibodies as serum

- biomarkers for cardiac disorders. *Journal of Molecular and Cellular Cardiology*, *143*, 145-158.
- Su, G., Sun, G., Liu, H., Shu, L., & Liang, Z. (2018). Downregulation of miR-34a promotes endothelial cell growth and suppresses apoptosis in atherosclerosis by regulating Bcl-2. *Heart and Vessels*, *33*(10), 1185-1194. doi:10.1007/s00380-018-1169-6
- Sun, C., Liu, H., Guo, J., Yu, Y., Yang, D., He, F., & Du, Z. (2017). MicroRNA-98 negatively regulates myocardial infarction-induced apoptosis by down-regulating Fas and caspase-3. *Scientific Reports*, *7*(1), 7460. doi:10.1038/s41598-017-07578-x
- Tabas, I., & Bornfeldt, K. E. (2020). Intracellular and Intercellular Aspects of Macrophage Immunometabolism in Atherosclerosis. *Circulation Research*, *126*(9), 1209-1227. doi:10.1161/CIRCRESAHA.119.315939
- Tan, M., Yin, Y., Ma, X., Zhang, J., Pan, W., Tan, M., . . . Li, H. (2023). Glutathione system enhancement for cardiac protection: pharmacological options against oxidative stress and ferroptosis. *Cell Death & Disease*, *14*(2), 131. doi:10.1038/s41419-023-05645-y
- Thygesen, K., Alpert, J. S., White, H. D., Jaffe, A. S., Apple, F. S., Galvani, M., . . . Al-Attar, N. (2007). Universal definition of myocardial infarction. *Circulation*, *116*(22), 2634-2653. doi:10.1161/circulationaha.107.187397
- Tibaut, M., & Petrovič, D. (2016). Oxidative Stress Genes, Antioxidants and Coronary Artery Disease in Type 2 Diabetes Mellitus. *Cardiovasc Hematol Agents Med Chem*, *14*(1), 23-38. doi:10.2174/1871525714666160407143416
- Treiber, T., Treiber, N., & Meister, G. (2019). Regulation of microRNA biogenesis and its crosstalk with other cellular pathways. *Nature reviews Molecular cell biology*, *20*(1), 5-20.
- Tsai, N.-W., Chang, Y.-T., Huang, C.-R., Lin, Y.-J., Lin, W.-C., Cheng, B.-C., . . . Huang, C.-C. (2014). Association between oxidative stress and outcome in different subtypes of acute ischemic stroke. *BioMed research international*, *2014*.
- Tsao, C. W., Aday, A. W., Almarzooq, Z. I., Anderson, C. A. M., Arora, P., Avery, C. L., . . . Martin, S. S. (2023). Heart Disease and Stroke Statistics—2023 Update: A Report From the American Heart Association. *Circulation*, *147*(8), e93-e621. doi:10.1161/CIR.0000000000001123
- Tsikas, D. (2017). Assessment of lipid peroxidation by measuring malondialdehyde (MDA) and relatives in biological samples: Analytical and biological challenges. *Analytical Biochemistry*, *524*, 13-30. doi:<https://doi.org/10.1016/j.ab.2016.10.021>
- Tsutsui, H., Kinugawa, S., & Matsushima, S. (2011). Oxidative stress and heart failure. *American Journal of Physiology-Heart and Circulatory Physiology*, *301*(6), H2181-H2190. doi:10.1152/ajpheart.00554.2011
- Wang, W., & Kang, P. M. (2020). Oxidative Stress and Antioxidant Treatments in Cardiovascular Diseases. *Antioxidants*, *9*(12), 1292.
- Warren, C. F. A., Wong-Brown, M. W., & Bowden, N. A. (2019). BCL-2 family isoforms in apoptosis and cancer. *Cell Death & Disease*, *10*(3), 177. doi:10.1038/s41419-019-1407-6
- Wolf, P., Schoeniger, A., & Edlich, F. (2022). Pro-apoptotic complexes of BAX and BAK on the outer mitochondrial membrane. *Biochimica et Biophysica Acta (BBA) - Molecular Cell Research*, *1869*(10), 119317. doi:<https://doi.org/10.1016/j.bbamcr.2022.119317>
- World Heart Report* (2023). Retrieved from <https://world-heart-federation.org/resource/world-heart-report-2023/>
- Xu, S., Ilyas, I., Little, P. J., Li, H., Kamato, D., Zheng, X., . . . Weng, J. (2021). Endothelial Dysfunction in Atherosclerotic Cardiovascular Diseases and Beyond: From Mechanism to Pharmacotherapies. *Pharmacological Reviews*, *73*(3), 924-967. doi:10.1124/pharmrev.120.000096
- Zhang, H., Kolb, F. A., Jaskiewicz, L., Westhof, E., & Filipowicz, W. (2004). Single processing center models for human Dicer and bacterial RNase III. *Cell*, *118*(1), 57-68.



- Zhang, P., Huang, C., Liu, H., Zhang, M., Liu, L., Zhai, Y., . . . Yang, J. (2023). The mechanism of the NFAT transcription factor family involved in oxidative stress response. *Journal of Cardiology*. doi:<https://doi.org/10.1016/j.jjcc.2023.04.017>
- Zhang, T., Tian, F., Wang, J., Jing, J., Zhou, S. S., & Chen, Y. D. (2015). Atherosclerosis-Associated Endothelial Cell Apoptosis by MiR-429-Mediated Down Regulation of Bcl-2. *Cellular Physiology and Biochemistry*, 37(4), 1421-1430. doi:10.1159/000438511
- Zhang, X., Sessa, W. C., & Fernández-Hernando, C. (2018). Endothelial Transcytosis of Lipoproteins in Atherosclerosis. *Front Cardiovasc Med*, 5, 130. doi:10.3389/fcvm.2018.00130
- Zhao, L., Varghese, Z., Moorhead, J. F., Chen, Y., & Ruan, X. Z. (2018). CD36 and lipid metabolism in the evolution of atherosclerosis. *British Medical Bulletin*, 126(1), 101-112. doi:10.1093/bmb/ldy006
- Zhou, Z.-Y., Wu, L., Liu, Y.-F., Tang, M.-Y., Tang, J.-Y., Deng, Y.-Q., . . . Huang, L. (2023). IRE1 $\alpha$ : from the function to the potential therapeutic target in atherosclerosis. *Molecular and Cellular Biochemistry*. doi:10.1007/s11010-023-04780-6

30-8-23

ORIGINALITY REPORT

11%	6%	7%	2%
SIMILARITY INDEX	INTERNET SOURCES	PUBLICATIONS	STUDENT PAPERS

PRIMARY SOURCES

1	Submitted to Higher Education Commission Pakistan Student Paper	1%
2	www.science.gov Internet Source	1%
3	www.ncbi.nlm.nih.gov Internet Source	<1%
4	Sen-Mao Li, Huan-Lei Wu, Xiao Yu, Kun Tang, Shao-Gang Wang, Zhang-Qun Ye, Jia Hu. "The putative tumour suppressor miR-1-3p modulates prostate cancer cell aggressiveness by repressing E2F5 and PFTK1", Journal of Experimental & Clinical Cancer Research, 2018 Publication	<1%
5	Mingyuan Xu, Jiaqi Sun, Yijia Yu, Qianqian Pang, Xiaohu Lin, May Barakat, Rui Lei, Jinghong Xu. "TM4SF1 involves in miR-1- 3p/miR-214-5p-mediated inhibition of the migration and proliferation in keloid by	<1%